UC San Diego

UC San Diego Electronic Theses and Dissertations

Title

Cell-extrinsic effects of tumor endoplasmic reticulum stress on myeloid cells

Permalink

https://escholarship.org/uc/item/51k3m50m

Author

Mahadevan, Navin R.

Publication Date

2012

Peer reviewed|Thesis/dissertation

eScholarship.org Powered by the California Digital Library
University of California

UNIVERSITY OF CALIFORNIA, SAN DIEGO

Cell-extrinsic effects of tumor endoplasmic reticulum stress on myeloid cells

A dissertation submitted in partial satisfaction of the

requirements for the degree Doctor of Philosophy

in

Biomedical Sciences

by

Navin R. Mahadevan

Committee in charge:

Professor Maurizio Zanetti, Chair
Professor Stephen Hedrick
Professor Santosh Kesari
Professor Cornelis Murre
Professor Victor Nizet

2012

Copyright

Navin R. Mahadevan, 2012

All rights reserved.

The Dissertation of Navin R. Mahadevan is approved, and it is acceptable in quality and form for publication on microfilm and electronically:

_____

_____

_____

_____

_____

Chair

University of California, San Diego

2012

DEDICATION

To my teachers and mentors, all of them, whose guidance, wisdom, and kindness has brought me thus far

EPIGRAPH

"…mille e tre!"

--Leporello, *Don Giovanni*

"1729"

--Srinivasa Ramanujan/G.H. Hardy

TABLE OF CONTENTS

LIST OF FIGURES

ACKNOWLEDGEMENTS

The work presented in this thesis would not have been possible, nor nearly as fun, to complete without the help, guidance, and shenanigans of the members of the Zanetti lab over the last four years. I would especially like to thank Jeff, Veronika, and Antonio for having helped me immensely in every aspect of this work, from culturing cells, to putting up with my "ever-evolving" experimental designs, to having the patience to go through the seemingly infinite number of figure drafts. While many others may have pulled their (and my) hair out, you persevered, and this work stands as a testament to your ingenuity, curiosity, intelligence, and spirit. I also thank Xochitl, DeShon, Homero, Matt, Gonzalo, Sree, Alex, and Shruti for their ever-available advice and discussion from the big science questions to the often-annoying questions of the location of reagents. I must also thank my other mentors who set me on my current path in the first place, Andy and Jeremy. I will never forget almost becoming the first human experiment for stem cell transplantation, nor the spawning of Amphioxus on my birthday.

To my lovely Gen—who may know this work better than I do because of the countless times I have told you about it—thank you for your patience and enthusiasm through the long work days and ongoing science babble, especially in the face of negative results or paper rejections. It is in part through your strength and encouragement that I have this work to present. To my family, Kannan, Ma, and T.P.: thank you for putting up with my West Coast location and long pauses in communication. The salvation, relaxation, and rejuvenation I feel every time I am able to see you all define the word

home. To my WashU friends, especially the Beau 2 crew, you are in my heart as we continue to take over the world.

To Maurizio, we have made our own luck. We met through serendipity and the rest is history, of which only a measure is recorded here. Words cannot express enough my thanks for your guidance and mentorship, which were the perfect blend of sound advice, encouragement, freedom, and enthusiasm. You have shown me how to retain one's curiosity, *joie de vivre*, and humanity when pursuing scientific knowledge even through some of the most difficult circumstances. We came through it together. *Grazie mille*.

The Introduction and Conclusions, in part, have been published in the manuscript: Mahadevan, N.R. and Zanetti, M. Tumor stress inside out: Cell-extrinsic effects of the unfolded protein response in tumor cells modulate the immunological landscape of the tumor microenvironment. *J Immunol* 187(9):4403-9, 2011. The dissertation author was the primary author of this paper.

Initial Studies and Chapters 1 and 2, in part, have been published in the manuscript: Mahadevan, N.R., Rodvold, J., Sepulveda, H., Rossi, S., Drew, A., and Zanetti, M. Transmission of ER stress and pro-inflammation from tumor cells to myeloid cells. *Proc Natl Acad Sci USA*, 108(16):6561-6, 2011. The dissertation author was the primary investigator and author of this paper and the other authors helped perform the research and write the manuscript.

Chapters 3, 4, and 5, in part, have been submitted to *Science* under the title, "Cell-extrinsic effects of tumor ER stress imprint myeloid dendritic cells and impair $CD8^+$ T

cell priming," authored by, Navin R. Mahadevan, Veronika Anufreichik, Jeffrey Rodvold, Homero Sepulveda, and Maurizio Zanetti. The dissertation author was the primary investigator and author of this paper and the other authors helped perform the research and write the manuscript.

CURRICULUM VITAE

EDUCATION

2006- **University of California, San Diego** **San Diego, CA**

Department of Biomedical Sciences, Medical Scientist Training Program
2008-2012: PhD, Biomedical Sciences, 4.0 cumulative GPA
School of Medicine, Medical Scientist Training Program
2012-2014: MD (*expected*)
2006-2008: Preclinical Training

2005-2006 **Pera Lab, Monash Institute of Medical Research** **Melbourne, Australia**

Fulbright Scholar

2001-2005 **Washington University in St. Louis** **St. Louis, MO**

A.B Biology Summa cum laude, 3.87 cumulative GPA
Anthropology Minor
Italian Minor

PUBLICATIONS

Mahadevan, N.R., Anufreichik, V., Rodvold, J., Sepulveda, H., and Zanetti, M. (2011). Cell-extrinsic effects of tumor ER stress imprint myeloid dendritic cells and impair $CD8^+$ T cell priming. *In preparation*.

Rodvold, J., **Mahadevan, N.R.**, and Zanetti, M. Lipocalin 2 in Cancer: When Good Immunity Goes Bad. *Cancer Letters* 316(2):132-8, 2012.

Mahadevan, N.R. and Zanetti, M. Tumor stress inside out: Cell-extrinsic effects of the unfolded protein response in tumor cells modulate the immunological landscape of the tumor microenvironment. *J Immunol* 187(9):4403-9, 2011.

Mahadevan, N.R., Rodvold, J., Almanza, G., Fernández Pérez, A.F., Wheeler, C. M., and Zanetti, M. ER stress drives Lipocalin 2 upregulation in prostate cancer cells in an NF-κB-dependent manner. *BMC Cancer* 11(1):229, 2011.

Mahadevan, N.R., Rodvold, J., Sepulveda, H., Rossi, S., Drew, A., and Zanetti, M. Transmission of ER stress and pro-inflammation from tumor cells to myeloid cells. *Proc Natl Acad Sci USA* 108(16):6561-6, 2011.

Mahadevan, N.R., Fernandez, A., Rodvold, J., Almanza, G., and Zanetti, M. Tumor cells undergoing ER stress in vitro and in vivo activate transcription of pro-inflammatory cytokines. *J Inflammation Res* 3: 99-103, 2010.

Horton A.C., **Mahadevan N.R.**, Minguillon C., Osoegawa K., Rokhsar D.S., Ruvinsky I., de Jong P.J., Logan M.P., Gibson-Brown J.J. Conservation of linkage and evolution of developmental function within the Tbx2/3/4/5 subfamily of T-box genes: implications for the origin of vertebrate limbs. *Dev Genes Evol* 2008 218(11-12):613-28.

Mahadevan N.R., Horton A.C., Gibson-Brown, J.J. Developmental expression of the amphioxus Tbx1/10 gene illuminates the evolution of vertebrate branchial arches and sclerotome. *Dev Genes Evol* 2004 214(11):559-66.

Horton A.C., **Mahadevan N.R**., Ruvinsky We., Gibson-Brown, J.J. Phylogenetic analyses alone do not reveal whether genome duplication(s) occurred during early vertebrate evolution. *J Exp Zoolog Part B Mol Dev Evol.* 2003 Oct15;299(1):41-53.

ABSTRACT OF THE DISSERTATION

Cell-extrinsic effects of tumor endoplasmic reticulum stress on myeloid cells

by

Navin R. Mahadevan

Doctor of Philosophy in Biomedical Sciences

University of California, San Diego

Professor Maurizio Zanetti, Chair

The unfolded protein response (UPR) is an evolutionarily-conserved group of signaling pathways that eukaryotic cells use to adapt to periods of perturbed endoplasmic reticulum (ER) function caused by the accumulation of un/misfolded proteins the ER lumen. Tumor cells undergo a constitutive UPR to survive the ER stress-inducing *noxae* within their microenvironment, such as hypoxia and nutrient deprivation. Elements of the tumor UPR have been shown to be key cell-intrinsic mechanisms of tumor survival but only few reports have considered the cell-extrinsic influence of the tumor UPR. Tumor-infiltrating myeloid cells, such as macrophages and dendritic cells, are key players in the cell-extrinsic regulation of tumor growth. Upon entering the tumor microenvironment, however, these cells are polarized to an inflammatory/suppressive phenotype that exacerbate the pro-inflammatory nature of the tumor microenvironment while

concomitantly suppressing cell-mediated anti-tumor immune responses. However, the tumor-derived signals driving this mixed inflammatory/suppressive phenotype have yet to be elucidated.

Herein, we show that the tumor cell UPR can function in a cell-extrinsic manner by transmitting ER stress to myeloid cells that infiltrate the tumor microenvironment, a phenomenon we have termed TERS (transmissible ER stress). TERS-imprinted myeloid cells upregulate production of tumorigenic, inflammatory cytokines but also upregulate immunosuppressive markers, culminating in a pro-inflammatory/suppressive phenotype. In macrophages, TERS is sensed, in part, by TLR4. Furthermore, TERS-imprinted myeloid cells display a unique functional phenotype, upregulating costimulatory molecule expression, antigen-presentation machinery, while downregulating effective high-affinity antigen cross-presentation. We demonstrate that TERS-imprinted BMDC do not effectively prime $CD8^+$ T cells, causing activation without proliferation, in part due to increased arginase activity. $CD8^+$ T cells cross-primed by TERS-imprinted BMDC display a regulatory phenotype and abnormally highly splicing of *Xbp-1*. We also show that TERS-imprinted BMDC can also dominantly suppress the proper cross-priming function of normal bystander BMDC. Lastly, TERS-imprinted BMDC facilitate tumor growth *in vivo*, even promoting the transient escape of highly immunogenic tumor cells. Taken together, we demonstrate the *ab initio* generation of tumor-imprinted myeloid cells that have many of the inflammatory/suppressive characteristics of previously-described tumor-infiltrating myeloid cells and bring to the forefront the tumor UPR as a fundamental driver of myeloid cell polarization.

INTRODUCTION

As early as the mid-1800s, histological examination of neoplastic tissues revealed infiltration by inflammatory cells, suggesting a close association between tumor development and inflammatory processes (1). Recent studies have added molecular detail to these early observations, highlighting the role of tumor- and leukocyte-derived inflammation in promoting tumor growth. Master regulators of inflammation, such as NF-κB and STAT3, have been shown to be crucial for tumor growth and the tumorigenic roles of some of their downstream effectors including cytokines, chemokines, and growth factors have been elucidated. It is now appreciated that the immune landscape of the tumor microenvironment undergoes continuous dynamic remodeling, and successful tumor outgrowth is contingent upon subversion and escape from cell-extrinsic immune control (2). In addition to directly facilitating tumor growth, inflammatory signals in the tumor microenvironment can subvert the local immune response against cancer cells by inhibiting antigen presenting cell and $CD8^+$ T cell function, promoting T regulatory cell (Treg) differentiation, and hampering the development of T cell memory (3, 4). While much work has focused on the genetic underpinnings of tumor-derived inflammation, less consideration has been given to microenvironmental and metabolic factors that could initiate and sustain inflammation in the tumor microenvironment. Recent evidence suggests that pathophysiologic conditions unique to the tumor microenvironment initiate tumor cell stress signals which converge upon the endoplasmic reticulum (ER), resulting in a condition termed ER stress (5). Here, we will discuss the ER stress response, its determinants in the tumor microenvironment, its newly appreciated role in tumorigenesis and new links between tumor cell ER stress and immune cells.

ER stress and the unfolded protein response

The ER is the initial checkpoint for the biosynthesis, folding, assembly, and modification of membrane-bound and secreted proteins in eukaryotic cells. Increase in physiological demand for protein folding or stimuli that disrupt the ability of proteins to fold cause the accumulation of un/misfolded proteins in the ER lumen, resulting in a condition known as ER stress. This activates intracellular signaling pathways known collectively as the unfolded protein response (UPR), which facilitates cellular adaptation to ER stress (6). In mammalian cells, the UPR is initiated by three ER membrane-bound sensors, IRE1α, ATF6, and PERK, which in unstressed cells, are maintained in an inactive state through luminal association with the ER chaperone molecule GRP78 (78 kDa glucose-regulated protein) (7). When a cell experiences ER stress, GRP78 disassociates from each of the three sensor molecules to preferentially bind un/misfolded proteins, allowing each sensor to activate downstream signaling cascades, which act to normalize protein folding and secretion (8).

Upon disassociation from GRP78, IRE1α autophosphorylates, thereby activating its endonuclease function to remove a 26 bp-segment from the *Xbp-1* mRNA transcript. Translation of the shortened transcript yields an Xbp-1 isoform (Xbp-1s) (9) that acts as a powerful driver of the production of various ER chaperone proteins which function to restore ER homeostasis by promoting proper protein folding, maturation, secretion, and degradation. Xbp-1s also promotes the transcription of *GRP78*, *XBP-1*, thus establishing a positive feedback loop (10). Activated ATF6 translocates to the Golgi where it is cleaved into its functional form, which acts in parallel with XBP-1s to restore ER homeostasis (11). Upon release from GRP78, PERK phosphorylates eIF2α, resulting in

the selective inhibition of translation (12), effectively reducing ER client protein load. If ER stress persists, downstream signaling from PERK via ATF4 can also activate the transcription factor, CHOP, which can initiate apoptosis (13). A schematic of the UPR is shown in Figure 1.

The tumor microenvironment harbors stimuli that elicit the UPR in tumor cells

The tumor microenvironment differs markedly from that of normal tissues. Most notably, tumors lack a well-developed blood supply, which, coupled with the rapid proliferation of tumor cells, leads to hypoxia, decreased glucose and amino acid supply, and low extracellular pH (5). These microenvironmental stressors all elicit UPR activation, which is well documented in solid tumor cells of diverse histological origin. Compounding these extrinsic *noxae* are tumor-intrinsic stressors, such as errors in the biosynthesis of glycoproteins and lipids (14, 15), and viruses (16), which collectively induce ER stress.

Hypoxia

Several lines of evidence indicate that hypoxia activates the UPR in tumor cells. Microarray analysis of *ras* and *c-myc* transformed mouse fibroblasts exposed to severe hypoxia *in vitro* reveal that multiple elements of the UPR, including *Chop*, *Grp78*, *Xbp-1*, and *Atf4*, are significantly upregulated compared to normoxic cells. Human fibrosarcoma and lung carcinoma cells upregulate GRP78 and increase XBP-1 splicing under hypoxic conditions *in vitro* (17, 18). Transgenic mice with spontaneous mammary carcinogenesis in which *Xbp-1* splicing is marked by luciferase expression, showed that Xbp-1s

bioluminescence correlates strongly with increasing tumor hypoxia and colocalizes with CA-9, a marker of hypoxia. In human colon cancer cells, hypoxia induces PERK-dependent eIF2α phosphorylation and ATF4 production (19).

Glucose Deprivation

Tumors grow in glucose-poor environments although tumor cells rapidly take up and utilize glucose. Thus, while PET measurements of 2-fluorodeoxyglucose (2-FDG) uptake in various human cancer cell lines, human xenograft models, and patient tumors *in vivo*, indicate that glucose entry (20-23), poor vascularization and the high rate of tumor cell glycolysis combine to severely limit the glucose available to tumor cells (24-26). It has been long known that glucose deprivation activates cellular stress responses. The GRP protein family, including GRP78, was originally discovered because of its upregulation in response to glucose deprivation (27). Further experiments in human colon cancer, fibrosarcoma, and lung carcinoma cell lines have shown that glucose deprivation and/or treatment with 2-deoxyglucose (2-DG), which mimics glucose deprivation, induces GRP78, and truncation of ATF6 and *XBP-1* to their active forms (17, 28, 29). Treatment of human colon cancer and renal carcinoma cell lines with 2-DG also induces eIF2a phosphorylation, ATF4, and ATF6/XBP1 activation (29). eIF2α phosphorylation and ATF4 activation are impaired in $PERK^{-/-}$ cells deprived of glucose (30), indicating that PERK induces downstream effectors in response to glucose deprivation. In their *in vivo* model of microenvironment-driven tumor cell ER stress, Spiotto et al. (31) demonstrated that Xbp1-luciferase activity in spontaneous mammary tumors significantly increased when tumor-bearing mice were treated with 2-DG, and that glucose deprivation

of tumor cells *ex vivo* caused a dramatic increase in Xbp1-luciferase expression. Taken together, these findings suggest that the low glucose in the tumor microenvironment, which arises as a result of poor vascularization and the high glycolytic rate of tumors, and hypoxia, are physiologically relevant inducers of ER stress in tumors *in vivo*.

The UPR is activated in tumors and is essential for tumorigenesis

Accumulating evidence demonstrates UPR activation in tumor cells and its critical role in solid tumor growth and progression. Primary human tumor cells of several origins, including breast (32), lung (33), liver (34), colon (35), prostate (36), and brain (37) have been shown to upregulate UPR pathways, including GRP78, ATF6, and XBP-1 splicing, whereas peritumoral areas do not. Additionally, in primary human melanoma, liver, and breast cancer specimens, the level of GRP78 positively correlates with tumor progression (32, 34, 38).

The functional link between the UPR and tumorigenesis was initially suggested by the finding that silencing of Grp78 in mouse fibrosarcoma cells inhibited growth in an *in vivo* syngeneic transplantation model due, in part, to increased tumor cell-specific T memory cell generation (39). Additionally, human glioma cells expressing a siRNA against *GRP78* display decreased growth rate *in vitro* (37). The essential role of GRP78 in tumorigenesis was confirmed when it was shown that *Grp78* hemizygous mice crossed with *MMTV-PyT* heterozygous transgenic mice display significantly decreased breast tumor proliferation, survival, and angiogenesis compared to *Grp78+/+, PyT* mice (40). Similarly, the conditional homozygous knockout of *Grp78* in the prostates of mice with *Pten* inactivation protects against prostate cancer growth (41).

More recent work has demonstrated that UPR signaling pathways downstream of Grp78 facilitate tumor growth. Human glioma cells expressing a dominant-negative IRE1α mutant display a decreased growth rate and impaired angiogenesis compared to cells transfected with empty vector when orthotopically transplanted into immunodeficient mice (17). Mouse fibroblasts deficient in *Xbp1* are more sensitive to hypoxic stress *in vitro* than wild type cells, and do not grow as tumors when injected into SCID mice. Consistent with these findings, fibroblasts expressing a siRNA against *Xbp-1* show a significant delay in tumor growth, are smaller than wild-type tumors, and exhibit decreased angiogenesis as compared to cells expressing non-specific control siRNAs or empty vector (18, 42). The importance of the IRE1α-XBP-1 signaling pathway to tumor growth has been confirmed in human tumor cells. siRNA inhibition of *Xbp-1* in human fibrosarcoma cells also inhibits their growth and angiogenesis in a xenograft model. Overexpression of XBP-1s in human fibrosarcoma cells expressing a dominant-negative IRE1α mutant rescues xenograft angiogenesis and XBP-1s expression positively correlates the endothelial cell marker, CD31, in human pancreatic adenocarcinoma specimens (42), PERK signaling also supports tumor growth during conditions of ER stress. The inactivation of ER stress signaling by mutations of PERK, or by the introduction of a dominant-negative PERK, in mouse fibroblasts and human colon cancer cells, results in tumors that are smaller, grow less rapidly, and display impaired angiogenic ability, as compared to their normal counterparts when grafted into immunodeficient mice. (19, 43) Taken together, these results underscore the key contribution of UPR in the growth and progression of solid tumors of diverse origins.

Notably, the fact that the UPR is specifically upregulated in most many tumors is driving the rational development of new anti-cancer therapies. Their mechanism involves inhibiting ER stress response pathways, which prevents tumor cells from coping with endogenous, constitutive ER stress due to microenvironmental stimuli (e.g. most solid tumors) or to high basal ER stress due to high ER protein load (e.g. myeloma, pancreatic cancer), leading to cell death. These therapies can be combined with drugs that further induce ER stress; together, these strategies aim to overload the ER while simultaneously limiting the tumor cell's ability to adapt via the UPR, leading to tumor regression (44, 45).

The UPR intersects with cellular pro-inflammation

In addition to coping with an increased un/misfolded protein load in the ER, the UPR activates a pro-inflammatory cascade with tumor-promoting and cell-survival properties. One of the key inflammatory regulators inducible by the UPR is NF-κB (46). Each of the three UPR signaling pathways activates NF-κB translocation to the nucleus via distinct mechanisms and consequent inflammatory gene transcription. PERK leads to NF-κB activation via a unique mechanism in which translational inhibition reduces the ratio of the IκB to NF-κB thus permitting the nuclear migration of NF-κB and transcription of downstream inflammatory genes (47, 48). Upon autophosphorylation, IRE1α forms a complex with tumor-necrosis factor-α (TNF-α)-receptor-associated factor 2 (TRAF2) at its cytosolic domain, and the IRE1α-TRAF2 complex mediates direct IκB phosphorylation via IκB kinase (IKK), which leads to NF-κB activation. Ire1α-deficient

mouse fibroblasts under ER stress display reduced NF-κB activation and downstream TNF-α production (49). Most recently, ATF6 was shown to participate in NF-κB activation in an AKT-dependent manner (50). That the UPR activates NF-κB via three independent mechanisms suggests that the ER stress response is a key regulator of cellular inflammation.

The UPR can also activate the JNK-AP-1 pathway of inflammation. The IRE1α-TRAF2 complex, aided by ASK and AIP (51), can recruit JNK, which phosphorylates the transcription factor, AP-1, leading to inflammatory gene expression. Supporting this model, IRE1α- or AIP-deficient fibroblasts under ER stress fail activate JNK and downstream inflammatory responses (51, 52).

Crosstalk between the UPR and inflammatory pathways is not unidirectional. Inflammatory cytokines and reactive cell metabolites can themselves induce the UPR. For instance, TNF-α activates IRE1α, ATF6, and PERK in mouse fibrosarcoma cells by inducing the accumulation of reactive oxygen species (ROS) (53). Additionally, IL-6, IL-1β, and LPS activate the UPR in the liver *in vivo* (54). Furthermore, the UPR can cause the accumulation of, and be induced by, ROS, which have been shown to induce phosphorylation of IκB in T cell lymphoma and cervical cancer cells, permitting NF-κB-dependent gene transcription (55). Though the UPR has antioxidant function via PERK/ATF4/NRF2 signaling (56), prolonged ER stress can cause the accumulation of ROS via several mechanisms: 1) accumulation of misfolded proteins causes Ca^{2+} leak from the ER which stimulates mitochondrial ROS production, which itself can increase ER Ca^{2+} depletion, 2) depletion of ATP to fuel protein folding induces mitochondrial

respiration, whose byproducts include ROS, and 3) formation of ROS as the consequence of formation and breakage of disulfide bond and during normal protein folding (57). Notably, limiting ROS accumulation *in vivo* using an antioxidant attenuates ER stress (58), indicating that ROS themselves also elicit the UPR.

The phenotype and immunosuppressive effects of tumor-infiltrating myeloid cells

Tumor-infiltrating myeloid cells can account for up to 30% of leukocytes in tumors (59) and are key players in the cell-extrinsic regulation of tumor growth. Because of their crucial role in priming adaptive immunity, their subversion by tumor cells represents one of the key mechanisms by which tumors escape immune control. The tumor-infiltrating myeloid population was initially characterized as heterogenous, comprising $CD11b^{+}/Gr1^{+}$ myeloid-derived suppressor cells (MDSC), which contain, and may be precursors to (60), subpopulations of $CD11b^{+}/Gr1^{+}/F480^{+}$ tumor-associated macrophages (TAM) and $CD11b^{+}/CD11c^{+}$ tumor-infiltrating dendritic cells (TIDC) (61). Because of their ability to inhibit T cell responses *in vitro* and *in vivo* (62, 63), and the initial characterization of their phenotype as $IL\text{-}10^{+}/IL\text{-}12^{-}$ coupled with low levels of costimulatory molecules and antigen presentation machinery, it was proposed that tumor-associated CD11b+/Gr1+ myeloid cells possessed an anti-inflammatory and suppressive (M2) phenotype (59). TIDC were first characterized as having an immature phenotype characterized by low levels of MHC Class I and II, and co-stimulatory molecule (CD86/CD80) expression, which was assumed to be responsible for the dysfunctional T cell priming and induction of anergy observed by these cells (64).

Evidence has accumulated that implicates tumor- and host-derived inflammatory processes in the accumulation and activity of MDSC (for a extensive review on the topic, see (65)). The inflammation-associated, pro-angiogenic factor VEGF stimulates the generation of MDSC in a paracrine and autocrine manner (66, 67). Tumor- and host-derived IL-1β and IL-6 cause increased MDSC burden, and increased MDSC suppressive activity and tumor outgrowth is associated with tumor-derived IL-1β (68, 69). COX-2-derived PGE_2 secreted by tumor cells polarize myeloid cells to a suppressive phenotype (70, 71). Collectively, these data may also explain recent findings that myeloid cells within the tumor microenvironment can have an inflammatory/activated phenotype while concurrently inhibiting anti-tumor immune responses and aiding tumor growth. For instance, in tumor-associated myeloid cells, generation of reactive oxygen species crucial for the inhibition of T cell responses can occur via arginase, a classical M2 marker, but also via iNOS, an inflammatory (M1) marker (62, 72). Furthermore, as discussed below, tumor-derived myeloid cells produce inflammatory cytokines such as IL-6, IL-23, and TNF-α that play key roles in tumor growth and in regulating anti-tumor immunity (3). More recently, it has been found that TIDC in melanoma (73), lung carcinoma (74), and breast cancer (75) express high levels of MHC Class I/II, CD80, and CD86, yet they still inhibit anti-tumor $CD8^+$ T cell responses *in vitro* and *in vivo* due to inadequate antigen presentation and arginase production (74-76). Taken together, these results underscore a heretofore-unappreciated phenotype of tumor-associated myeloid cells as both inflammatory and suppressive (77). The tumor-derived signals driving this mixed inflammatory/suppressive phenotype have yet to be elucidated.

Whereas only few studies have investigated antigen processing and presentation in tumor-associated myeloid cells, studies have shown that inhibition of TCR engagement of specific peptide/MHC complexes by tumor-associated myeloid cells can occur via ROS-mediated nitration (62, 78). Antigen-independent mechanisms of myeloid cell-mediated inhibition of T cell function include local depletion of L-arginine via arginase upregulation or ROS production, release of immunomodulatory cytokines such as TGF-β (60, 75), local cysteine depletion (79), and induction of L-selectin downregulation on T cells (80).

UPR involvement in antigen presentation

Jamora et al. (39) first showed that *Grp78*-deficient fibrosarcoma cells evoke a more robust T memory cell response resulting in rejection of tumor cells with low immunogenicity. This finding suggested the intriguing, but little-explored, possibility that UPR signaling in tumor cells can impinge upon tumor antigen presentation and the host anti-tumor immune response. We have shown that while B cells mounting an UPR following accumulation of a KDEL-retained protein in the ER upregulate MHC Class II and costimulatory molecules (81), they present decreased levels of high affinity peptide complexed to MHC Class II. Similarly, mouse thymoma cells under palmitate or glucose deprivation-induced ER stress decrease transgenic ovalbumin antigen presentation on MHC Class I (82). These findings begin to suggest that antigen presenting cells under ER stress undergo remodeling of the processing machinery yielding decreased presentation of high affinity immunodominant peptides and increased presentation of subdominant or low affinity peptides. This was the conclusion of a study in human cancer cells treated

with the histone deacetylase inhibitor trichostatin A, which also upregulates ER stress response genes while diminishing tapasin (83), a chaperone molecule involved in quality control of MHC I/peptide complexes in the ER (84). The relationship between ER stress and tapasin is underscored by findings demonstrating that specific induction of the UPR using thapsigargin, a highly potent inducer of ER stress, causes downregulation of tapasin transcription in lymphoma cells (81). Thus, a UPR response in tumor cells and in antigen presenting cells may have the effect of rearranging the hierarchy of the immunopeptidome.

UPR-linked effects on immunoregulatory signals

The UPR is linked to the production of several inflammatory, tumorigenic cytokines: IL-6, IL-23, and TNF-α. A microarray analysis of mouse lymphoma cells under *in vitro* pharmacological ER stress reveals transcriptional upregulation of multiple inflammatory genes, including *Il-6*, *Il-23p19*, *Tnf-α*, *Tlr2*, and *Cebpb* (81). Furthermore the levels of *in vivo* ER stress, as measured by *Grp78* expression, correlate with *Il-6*, *Il-23p19*, and *Tnf-α* transcription in murine prostate cancer cells growing in a heterotopic transplantation model (85).

CHOP is necessary for IL-23 production by dendritic cells (86), and IL-6 and TNF-α by macrophages (87). Redundant roles for IRE1α and PERK signaling in IL-6 and TNF-α production in macrophages have been reported (87, 88). ChIP analysis also reveals that XBP-1s binds to the promoters of the *Il-6* and *Tnf-α*; congruently, Ire1α- or Xbp1-deficient macrophages display impaired IL-6 and TNF-α production in response to

pharmacological ER stress and infectious TLR agonism (88). The UPR also synergizes with TLR4 agonism to result in robust IL-23 secretion by macrophages (89). Interestingly, the UPR in cancer cells also upregulates Lipocalin 2 (Lcn2) (90), an innate immune inflammatory molecule whose first described function is the prevention of iron scavenging by bacterial siderophores (91). Notably, spontaneous breast cancer in mice showed a decreased rate of progression in *Lcn2*-deficient mice (92, 93).

UPR-linked pro-inflammatory mediators (94) in the tumor microenvironment facilitate tumor growth and regulate immune function (3). For example, inhibition of the NF−κB by ablation of IKKβ in liver macrophages results in loss of TNF-α and IL-6 production, which in turn, impairs tumor growth (95). Macrophage-specific deletion of IKKβ leads to decreased production of PGE_2 and IL-6, resulting in reduced incidence of colitis-associated colorectal tumors (96). In a model of lung cancer, IL-6 and TNF-α produced by myeloid cells in response to tumor-derived versican (97) drive tumor growth and progression in a TLR2-dependent manner. IL-23 produced by TAM blocks $CD8^+$ T cell infiltration into tumors (98) and upregulates T regulatory cell differentiation in the tumor microenvironment (99).

Possible cell-extrinsic effects of the UPR on tumor-infiltrating immune cells

The UPR has thus far mostly been studied in the context of tumor-intrinsic signaling that sustains survival and proliferation. The new paradigm of an UPR signaling umbrella under which pro-inflammation in the tumor microenvironment originates, together with the key role of inflammation in determining the phenotypic and functional complexity of TAM and TIDC, raises the intriguing possibility that the tumor UPR may

impair host immune function in the tumor microenvironment in a cell-extrinsic manner.

As a first step to investigate this hypothesis, we have modeled the interaction between ER-stressed tumor cells and macrophages in the tumor microenvironment by culturing macrophages in the conditioned medium of murine cancer cells experiencing pharmacological or physiological ER stress *in vitro*. Surprisingly, J774 macrophages treated in this manner upregulate UPR signaling as well as production of pro-inflammatory molecules, including Il-6, Il-23, Tnf-α, CD86, Mip-1α, and Mip-1β (see Initial Studies). Given the tumorigenic nature of several of these cytokines, notably IL-6 and IL-23 (98, 100), as well as recent reports demonstrating that Xbp-1s and Chop are necessary for Il-6, Il-23, and Tnf-α production in macrophages, and that the Ire1-Xbp1 pathway synergizes with TLR2/4 signaling in macrophages (86, 88, 89), it is tempting to suggest that microenvironment-induced ER stress in tumor cells can be propagated to infiltrating myeloid cells, which may result in the sustained production of pro-inflammatory, tumorigenic cytokines thus molding the tumor microenvironment to favor tumor progression.

The consequences of tumor UPR-mediated derangement of antigen presenting cells, such as macrophages and dendritic cells, in the tumor microenvironment remain unknown. It is possible that via its cell-extrinsic cues, the tumor UPR may ultimately manifest its consequences in defective T cell priming. As noted above, one consequence of ER stress in antigen presenting cells is impaired peptide presentation in the presence of adequate costimulatory molecule expression. T cell dysfunction could also occur via antigen-independent mechanisms as the tumor UPR affects the cytokine and metabolic profile of the APC.

Concluding Remarks

The UPR is a stress-adaptation mechanism that functions to maintain ER homeostasis. The tumor microenvironment harbors multiple ER stress-evoking stimuli, including hypoxia and low glucose, and, as such, the tumor ER stress response has thus far been studied mostly in its capacity to aid tumorigenesis via cell-intrinsic mechanisms. Emerging evidence suggests that the ER stress response is a major modulator of cellular inflammation as it regulates NF-κB and the production of several tumorigenic, immunoregulatory cytokines. Furthermore, it has been found that the UPR may a role in myeloid cell antigen presentation. These findings together with evidence from this lab and others suggest that the tumor UPR may influence infiltrating myeloid cells in a cell-extrinsic manner, possibly resulting in immune subversion and tumor outgrowth.

The hypothesis of this dissertation is that tumor cells under ER stress can polarize myeloid cells via a cell-extrinsic mechanism to a phenotype that can promote tumor progression through $CD8^+$ T cell-independent and dependent mechanisms. This concept is founded upon data from our lab demonstrating that J774 macrophages cultured in medium conditioned by tumor cells under pharmacological and physiological ER stress mount an ER stress response (a phenomenon we term “transmissible” ER stress [TERS]), and activate production of tumorigenic, pro-inflammatory cytokines (see Initial Studies).

In this dissertation, we further extend this work by evaluating the effect of TERS on bone marrow-derived macrophages, testing candidate BMDM receptors that may sense TERS, examining the consequences of TERS on dendritic cells, evaluating the antigen-presentation and subsequent $CD8^+$ T cell priming capacity of TERS-imprinted

dendritic cells, and testing the functional effect of TERS-primed dendritic cells on tumor growth *in vivo.*

The Introduction, in part, has been published in the manuscript: Mahadevan, N.R. and Zanetti, M. Tumor stress inside out: Cell-extrinsic effects of the unfolded protein response in tumor cells modulate the immunological landscape of the tumor microenvironment. *J Immunol* 187(9):4403-9, 2011. The dissertation author was the primary author of this paper.

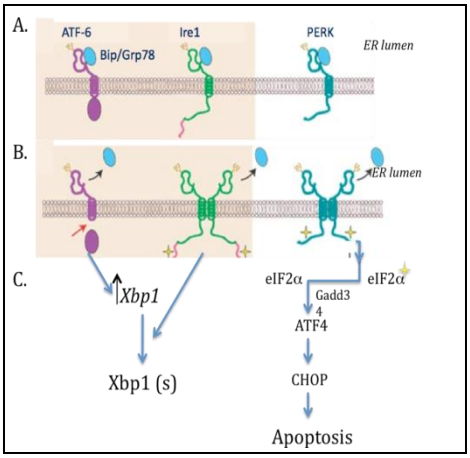

Figure 1. **Organization of the ER stress response elements (ERSE) and UPR.** BiP/Grp78 disassociation from IRE1, ATF6, and PERK activates their downstream signaling cascades. For more detail, refer to text.

INITIAL STUDIES. Development of models with which to study the cell-extrinsic influence of tumor ER stress on myeloid cells

The studies outlined here form the theoretical and experimental basis for the program of research described in this thesis. Briefly, they summarize the development of model systems used to study the cell-extrinsic consequences of tumor ER stress, discovery of "transmissible" ER stress (TERS) and concomitant pro-inflammation to macrophages, and demonstration of TERS *in vivo*.

1) Development of model systems in which to study the cell-extrinsic effects of tumor cell ER stress on macrophages.

To investigate the possible non-cognate influence of tumor cell ER stress on macrophages, we first developed an *in vitro* system of tumor ER stress using the canonical ER stress inducer, thapsigargin (Tg). Tg is a sesquiterpene lactone that specifically induces ER stress by inhibiting the sarco/endoplasmic reticulum Ca^{2+} ATPase (SERCA) (101). SERCA inhibition leads to the depletion of the ER Ca^{2+} store, resulting decreased chaperone function and accumulation of un/misfolded proteins, thus inducing ER stress. We found that the capacity of Tg to induce ER stress is comparable whether murine prostate cancer, TRAMP-C1 (TC1) cells are treated for 18 hrs continuously or for 2 hrs, washed and then cultured in fresh medium for an additional 16 hrs, suggesting that Tg needs not be continuously present in the medium to induce an ER stress response (Fig. 2). Thus, we used the 16 hr ER stress conditioned medium to explore possible non-cognate influences of ER stressed tumor cells on myeloid cells in a

model system in which cell-free ER stress conditioned medium is transferred to macrophages.

We also modeled a physiological tumor cell ER stressor glucose deprivation by culturing tumor cells in glucose-free medium containing 10% dialyzed fetal bovine serum (10000 MCWO), penicillin, streptomycin, and glutamine for 24 h before transfer to macrophages. Such treatment in three mouse tumor lines representative of prostate (TC1), melanoma (B16.F10), and lung carcinoma (Lewis Lung Carcinoma) resulted in a robust UPR as evinced by upregulation of *Grp78*, *Chop*, and *Xbp-1* as compared to cells grown in normoglycemic medium (Fig. 3).

2) Tumor cells transmit ER stress to macrophages, which concomitantly upregulate production of inflammatory, tumorigenic cytokines.

To investigate the possible non-cognate cell-extrinsic effects of tumor cells on immune cells in the tumor micronvironment, we cultured J774 macrophages in conditioned medium from Tg-treated TRAMP-C1 (TC1) murine prostate cancer cells. We found that J774 cells exposed to tumor ER stress conditioned medium (Tg c.m.) experienced ER stress, as indicated by upregulated transcription of UPR genes and a concomitant transcriptional upregulation of the tumorigenic inflammatory cytokines, *Il-6* and *Il-23p19* (Fig. 4A-C), whose increased secretion could be detected when TERS-primed macrophages were costimulated through TLR4 (Fig. 4E). Exposure to the ER stress conditioned medium also promoted the upregulation of the costimulatory molecule CD86, indicating macrophage activation.

To exclude the trivial explanation of Tg carryover, we analyzed the ER stress conditioned medium by mass spectroscopy and found it to contain no Tg within the limit of detection (< 1 ng/mL) (Fig. 5). Cell death was also ruled out as a contributing factor since Annexin V positivity in Tg-treated TC1 cells was comparable to that of vehicle-treated TC1 cells (Fig. 6A). Furthermore, J774 macrophages cultured in medium from TC1 cells treated with staurosporine to cause equivalent levels of cell death, failed to upregulate either the ER stress response or the pro-inflammatory cytokine genes (Fig. 6B). Finally, the effects could not be attributed to mycoplasma-induced activation because TC1 cells tested repeatedly negative for this pathogen (data not shown). These data suggest that the transmission of ER stress and pro-inflammation from tumor cells to macrophages is not due to Tg carryover, death, or contamination of TC1 "transmitter" cells.

Communication of ER stress and an attendant pro-inflammatory transcriptional response was also evident in macrophages cultured in the conditioned medium from other ER stressed tumor cell lines, B16.F10 (melanoma) and LLC (lung carcinoma) (Fig. 7). Thus, we concluded that tumor cell ER stress mediates a cell-extrinsic mechanism of influencing macrophages, causing them to mount an ER stress response and produce tumorigenic, pro-inflammatory cytokines.

3) A physiological model of tumor ER stress recapitulates TERS and attendant pro-inflammatory transcription in macrophages.

To verify that a physiological ER stressor found in the tumor microenvironment could evoke an ER stress response and pro-inflammatory cytokine transcription in

macrophages, we developed a model of *in vitro* ER stress based on glucose deprivation as shown in Fig. 3. Macrophages cultured for 24 h in glucose-deprived tumor (TC1, B16.F10, or LLC) supernatant displayed greater UPR and transcriptional inflammatory cytokine induction than macrophages grown in glucose-deprived medium alone (Fig. 8), confirming that a physiological microenvironmental tumor ER stressor can induce TERS and tumorigenic, pro-inflammation in macrophages.

4) Conditioned medium from ER-stressed tumor cells can induce ER stress *in vivo*.

To demonstrate that TERS could occur *in vivo*, we injected medium conditioned by Tg-treated tumor cells (TC1, B16.F10, or LLC) intraperitoneally into mice and assayed liver cells for an ER stress response 8 h later. We found that tumor ER stress conditioned medium induced a robust UPR in liver cells whereas vehicle conditioned medium and cell culture medium alone had no effect (Fig. 9) confirming that tumor cells under ER stress release factor(s) that can evoke an UPR in surrounding cells.

Summary

These studies uncovered a novel non-cognate, cell-extrinsic mechanism by which tumor cells can influence macrophages, one that is initiated by tumor cell ER stress. We demonstrate that the medium conditioned by tumor cells under pharmacological and physiological ER stress is able to evoke an ER stress response in J774 macrophages, which is accompanied by upregulation of tumorigenic, pro-inflammatory cytokines. Finally, we demonstrate that tumor ER stress conditioned medium can transmit ER stress to cells *in vivo*. Taken together, the results suggest that the constitutive ER stress

response observed in tumor cells *in vivo* not only functions to promote cell-intrinsic tumor adaptation but could also polarize infiltrating myeloid cells to a pro-tumorigenic phenotype. The further work detailed in this dissertation explores this notion.

The section Initial Studies, in part, has been published in the manuscript: Mahadevan, N.R., Rodvold, J., Sepulveda, H., Rossi, S., Drew, A., and Zanetti, M. Transmission of ER stress and pro-inflammation from tumor cells to myeloid cells. *Proc Natl Acad Sci USA*, 108(16):6561-6, 2011. The dissertation author was the primary investigator and author of this paper and the other authors helped perform the research and write the manuscript

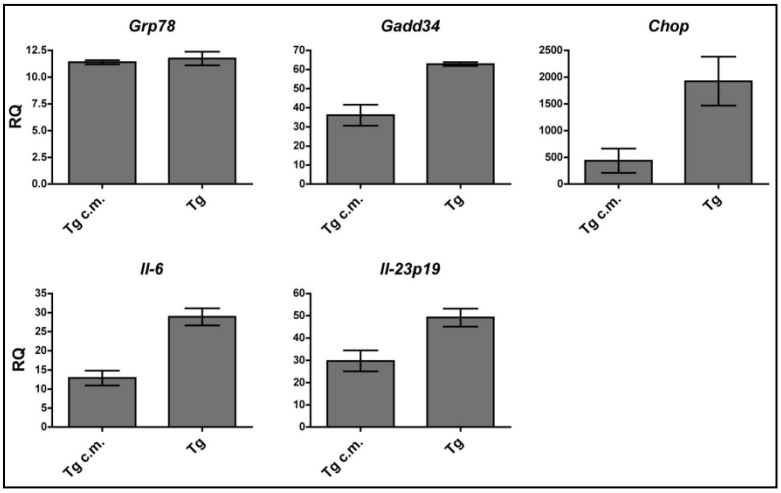

Figure 2. Modeling the non-cognate influence of tumor cell ER stress on macrophages. TC1 cells were treated with Tg (300 nM) for 2 h, washed, and cultured in fresh media for 16 h (Tg c.m.) or continuously for 18 hrs with Tg. RNA was isolated and analyzed by RT-qPCR for the UPR. Data columns indicate the fold difference in transcript level (RQ) between cells treated with Tg or an equal volume of vehicle control (100% ethanol) only. Error bars represent SEM of 2 biological replicates representative of 3 independent experiments.

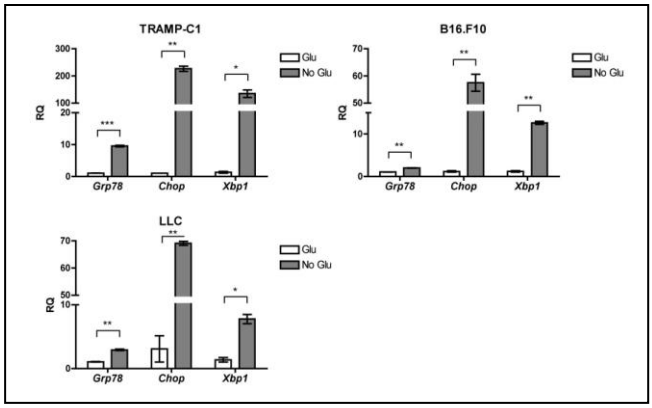

Figure 3. Glucose deprivation evokes an ER stress response in tumor cells. TRAMP-C1, B16.F10, and LLC tumor cells were cultured in growth medium lacking glucose (No Glu) or normoglycemic medium (Glu) for 24 h after which RNA was isolated and the ER stress response interrogated by RT-qPCR. Columns indicate the fold increase in transcript level (RQ) of each treatment group. The value of a normoglycemic control was set arbitrarily to 1 for each tumor cell line. Error bars represent SEM of 2 biological replicates. $*P < 0.05$, $**P < 0.01$, $***P < 0.001$, unpaired, two-tailed *t* test.

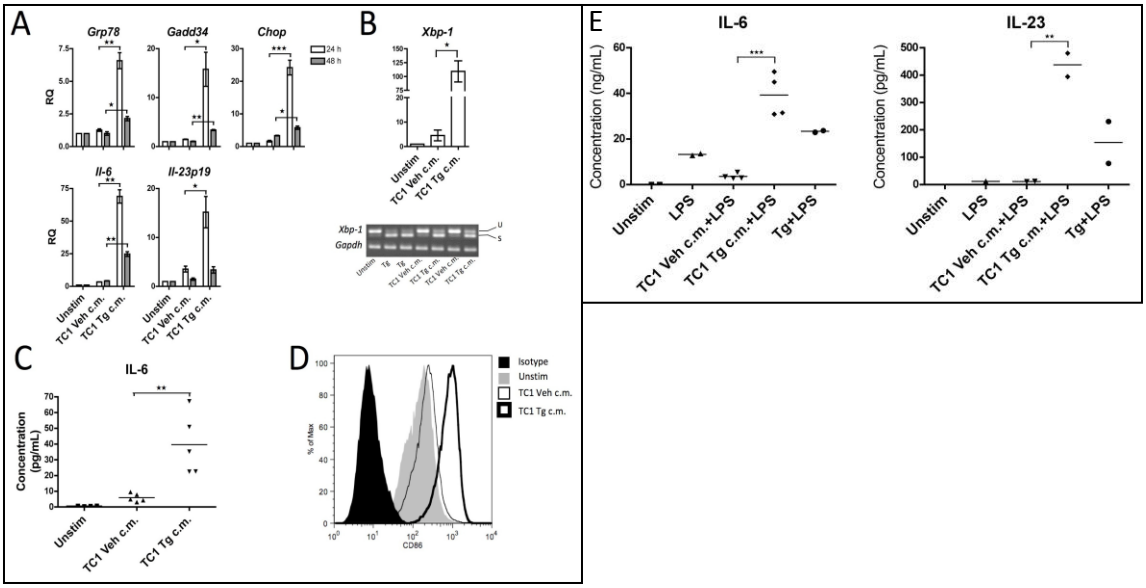

Figure 4. Macrophages experience "transmissible" ER stress and pro-inflammatory cytokine gene production. (**A-B**) J774 macrophages were cultured in conditioned medium of ER stressed TC1 cells (TC1 Tg c.m.), control TC1 cells (TC1 Veh c.m.), or culture medium alone (Unstim) for 24 or 48 hrs. RNA was isolated and analyzed by RT-qPCR for UPR activation and pro-inflammatory cytokine gene transcription. Columns indicate the fold increase in transcript level (RQ) of each treatment group. The value of unstimulated controls was set arbitrarily to 1. Error bars represent SEM of 2-5 independent experiments. * $P < 0.05$, ** $P < 0.01$, *** $P < 0.001$, unpaired, two-tailed *t* test. (**C**) J774 supernatants from the 24 and 48 hr timepoints were analyzed by the multiplex cytometric bead assay for presence of IL-6. ** $P < 0.01$, unpaired, two-tailed *t* test. (**D**) Flow cytometry analysis of J774 macrophages treated for48 h. Results are representative of 3 independent experiments. (**E**) J774 macrophages were cultured in conditioned medium of ER-stressed TC1 cells (TC1 Tg c.m.), control TC1 cells (TC1 Veh c.m.), or culture medium alone, with LPS (100 ng/mL) for 18 hrs. Macrophages cultured in medium containing Tg (300 nM) plus LPS serves as a control. Macrophage supernatants were analyzed by cytometric bead array assay for presence of cytokines. ** $P < 0.01$, *** $P < 0.001$, unpaired, two-tailed *t* test.

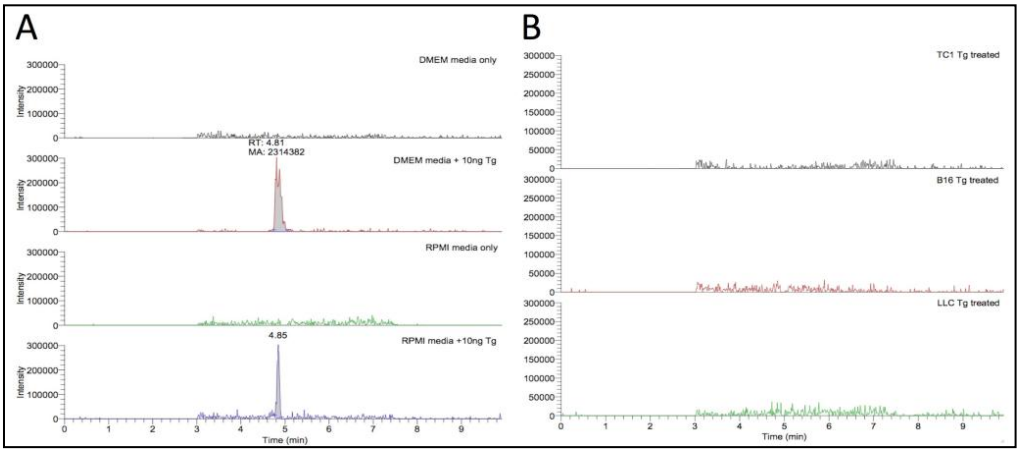

Figure 5. ER stress tumor conditioned media does not contain carryover thapsigargin. Samples of TC1, B16.F10, and LLC Tg c.m. medium were analyzed for presence of Tg (identified by cumulative product ions [m/z 513, 573, 612] from the protonated molecular ion parent [m/z 674]) by mass spectroscopy and compared against complete culture medium (RPMI or DMEM) spiked or not with 10 ng/mL Tg. Volumes analyzed were all 300 mL. (**A**) Ion-chromatograms of blank media (complete RPMI and DMEM) as well as blank media to which a known amount of Tg was added as positive control (equivalent to 10 ng/mL) (**B**) ion-chromatograms of TC1, B16.F10, and LLC Tg c.m.as annotated. The limit of detection was < 1 ng/mL.

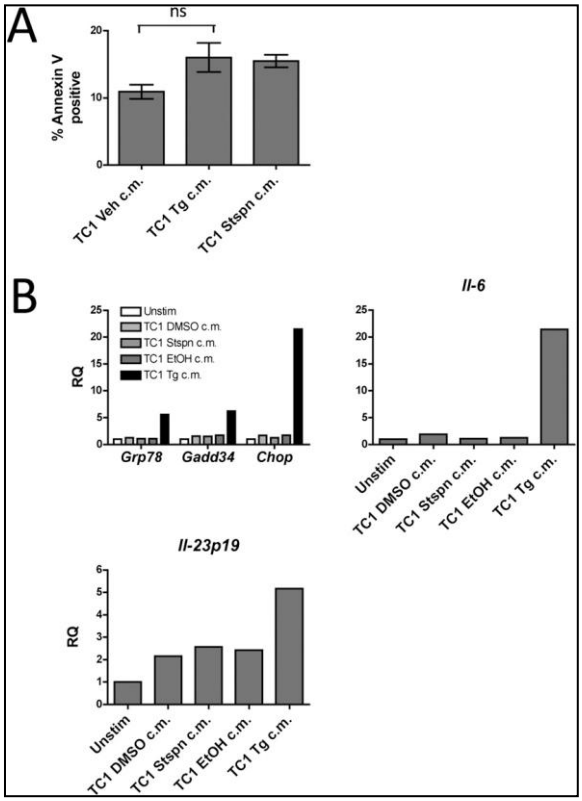

Figure 6. Cell death in Tg-treated TC1 cells does not account for "transmissible" ER stress and associated pro-inflammation in macrophages. (A) TC1 cells were treated with 300 nM Tg, 100 nM staurosporine (Stspn), or equal volumes of vehicle (100% EtOH and DMSO, respectively) and treated as indicated in Fig. 2, and analyzed for Annexin V positivity by flow cytometry. Error bars represent SEM of triplicate wells. ns = nonsignificant ($P > 0.05$, unpaired, two-tailed *t* test). **(B)** J774 macrophages were cultured in c.m. derived from TC1 treated with Tg (TC1 Tg c.m.), Stspn (TC1 Stspn c.m.), vehicles (100% EtOH or DMSO) only, or culture medium alone (Unstim) for 24 hrs. RNA was isolated and analyzed by RT-(q)PCR for UPR activation and pro-inflammatory cytokine transcription. Columns indicate the fold increase in transcript level (RQ) of each treatment group. The value of unstimulated controls was set arbitrarily to 1. Data shown is representative of two independent experiments.

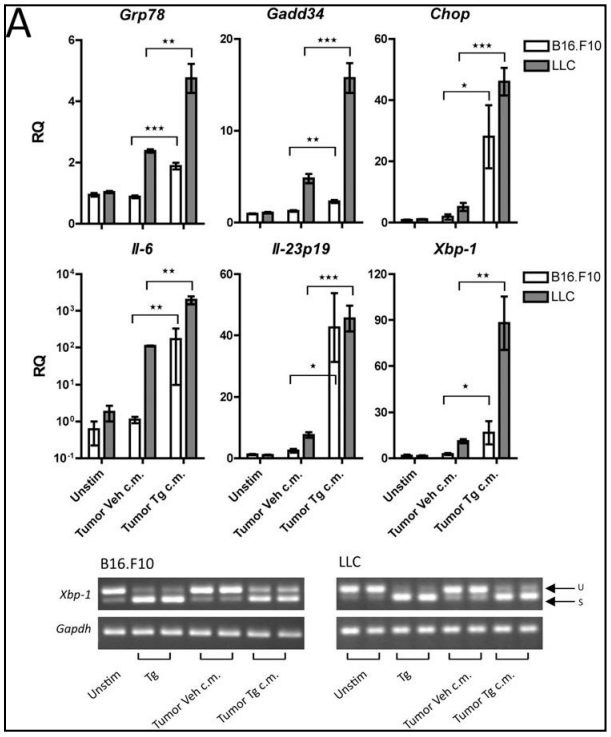

Figure 7. ER stressed conditioned medium from B16.F10 and LLC tumor cells also mediates transmissible ER stress and attendant pro-inflammation in macrophages. J774 macrophages were cultured in conditioned medium of ER stressed B16.F10 or LLC cells (B16.F10, LLC Tg c.m.), control cells (B16.F10, LLC Veh c.m.), or culture medium alone (Unstim) for 24 h. RNA was isolated and analyzed by RT-(q)PCR for UPR activation and pro-inflammatory cytokine gene transcription. Columns indicate the fold increase in transcript level (RQ) of each treatment group. The value of an unstimulated control was set arbitrarily to 1. Error bars represent SEM of 2-4 biological replicates. **P* < 0.05, ***P* < 0.01, ****P* < 0.001, unpaired, two-tailed *t* test. Abbreviations: u = unspliced; s = spliced.

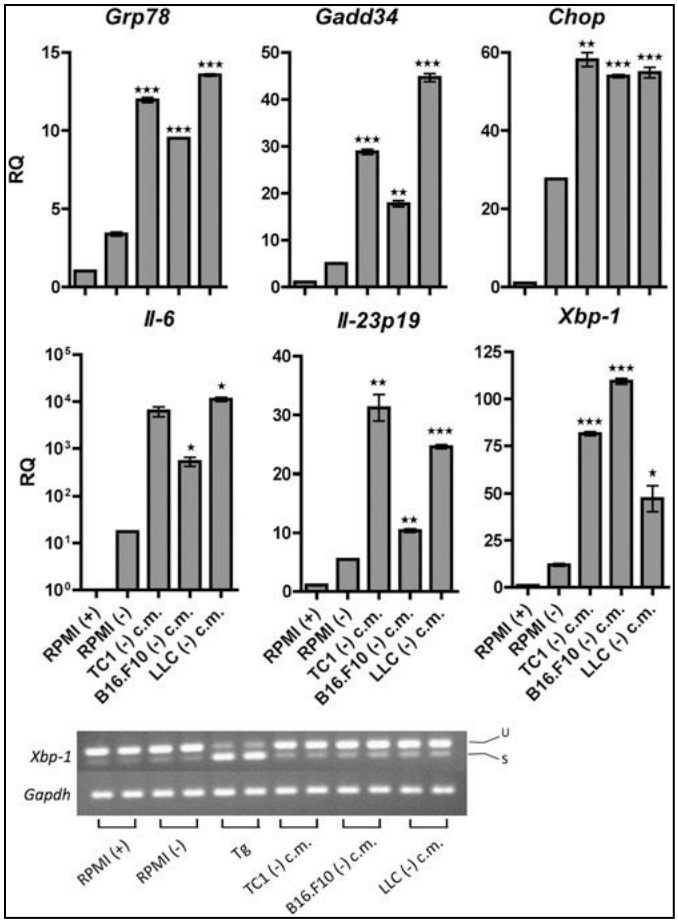

Figure 8. Medium conditioned by tumor cells under physiological ER stress transmits ER stress and pro-inflammation to macrophages. J774 macrophages were cultured in conditioned medium of glucose-deprived tumor cells (TC1, B16.F10, LLC (-) c.m.), or culture medium with [RPMI (+)] or without [RPMI(-)] glucose for 24 hrs. RNA was isolated and analyzed by RT-(q)PCR for UPR activation and pro-inflammatory cytokine gene transcription. Columns indicate the fold increase in transcript level (RQ) of each treatment group. The value of a RPMI (+) control was set arbitrarily to 1. Error bars represent SEM of 2 biological replicates. $*P < 0.05$, $**P < 0.01$, $***P < 0.001$, unpaired, two-tailed *t* test. Test samples' gene expression was compared to the gene expression of RPMI (-) cells.

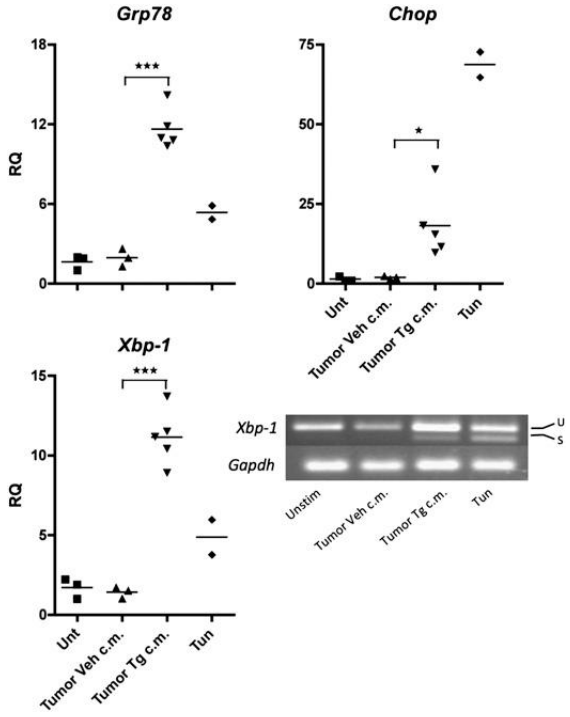

Figure 9. Tumor ER stress conditioned medium elicits an ER stress response *in vivo*. 10X conditioned medium of ER stressed (Tumor Tg c.m.) or control (Tumor Veh c.m.) tumor cells in 1 mL was injected i.p into C57BL/6 mice. Tunicamycin-treated (Tun, 2 mg/kg) and untreated (Unt) mice served as controls. Two mice were given TC1 Tg c.m. or B16.F10 Tg c.m., respectively and one received LLC Tg c.m. Control conditioned medium derived from each cell line was injected into one mouse each (three). Livers were harvested 8 h after injection. RNA was isolated and analyzed by RT-(q)PCR for UPR activation. Columns indicate the fold increase in transcript level (RQ) of each treatment group. The value of a single untreated control was set arbitrarily to 1. *$P < 0.05$, ***$P < 0.001$, unpaired, two-tailed *t* test. Abbreviations: u = unspliced; s = spliced.

.

CHAPTER 1. Exploring the cell-extrinsic influence of ER-stressed tumor cells on bone marrow-derived macrophages (BMDM)

Rationale

We have previously shown that tumor ER stress conditioned media ($TERS^{cm}$) polarizes J774 macrophages to undergo "transmissible ER stress" (TERS) and upregulate pro-inflammatory cytokine production. Here, we aimed to determine whether BMDM, a physiological model of tumor-infiltrating macrophages, are subject to transmissible ER stress and associated pro-inflammatory cytokine production.

Results

We determined that bone marrow-derived macrophages (BMDM) are also susceptible to "transmissible ER stress" using the Tg-induced ER stress and the supernatant transfer system already described. Similar to J774 macrophages, $CD11b^{+}$ BMDM cultured in $TERS^{cm}$ experienced ER stress, and *Il-6*, *Il-23p19*, tumor necrosis *TNF-α* transcriptional up-regulation (Fig. 10A), as well as CD86 activation (Fig. 10B). BMDM cultured in tumor ER stress-conditioned medium also secreted large amounts of two inflammatory chemokines, macrophage inflammatory protein-1α (MIP-1α) and MIP-1β (see Ch. 2, Fig. 13D), which themselves are known to induce the synthesis and release of IL-6 and TNF-α (102). Taken together, the results show that ER-stressed tumor cells release a soluble factor (or factors) that activates macrophages and initiates an ER stress response along with transcriptional activation and secretion of proinflammatory cytokines and chemokines.

In an attempt to distinguish TERS^{cm}-imprinted BMDM into M1 (pro-inflammatory) or M2 (anti-inflammatory/suppressive) cells (59), we found that they up-regulate CD86 (Fig. 10B, Fig. 11A), but fail to modulate CD64, CD16/32, or CD14 expression (Fig. 11A). Additionally, they do not up-regulate transcription of *Il-10* (Fig. 11B). Confirming their identity as tumor-associated macrophages, receiver macrophages up-regulate arginase transcription (although variably) (Fig. 11C), indicating they may have a mixed pro-inflammatory/suppressive phenotype, which is summarized in Figure 12.

Chapter 1, in part, has been published in the manuscript: Mahadevan, N.R., Rodvold, J., Sepulveda, H., Rossi, S., Drew, A., and Zanetti, M. Transmission of ER stress and pro-inflammation from tumor cells to myeloid cells. *Proc Natl Acad Sci USA*, 108(16):6561-6, 2011. The dissertation author was the primary investigator and author of this paper and the other authors helped perform the research and write the manuscript.

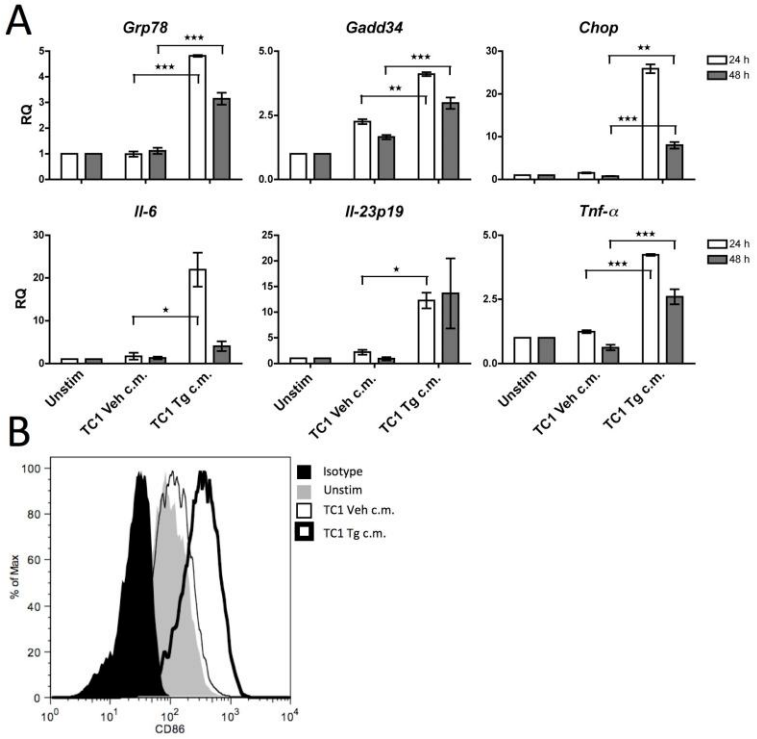

Figure 10. BMDM experience transmissible ER stress and proinflammatory cytokine gene transcription. BMDM were cultured in conditioned medium of ER stressed TC1 cells (TC1 Tg c.m.), control TC1 cells (TC1 Veh c.m.), or culture medium alone (Unstim) for 24 or 48 h. **(A)** RNA was isolated and analyzed by RT-qPCRfor UPR activation and proinflammatory cytokine gene transcription. Columns indicate fold increase in transcript level (RQ) of each treatment group. The value of unstimulated controls was set arbitrarily to 1. Error bars represent SEM of two to five independent experiments. **P* < 0.05, ***P* < 0.01, ****P* < 0.001, unpaired, two-tailed *t* test. **(B)** Flow cytometry analysis of BMDM treated as indicated for 48 h. Results are representative of three independent experiments.

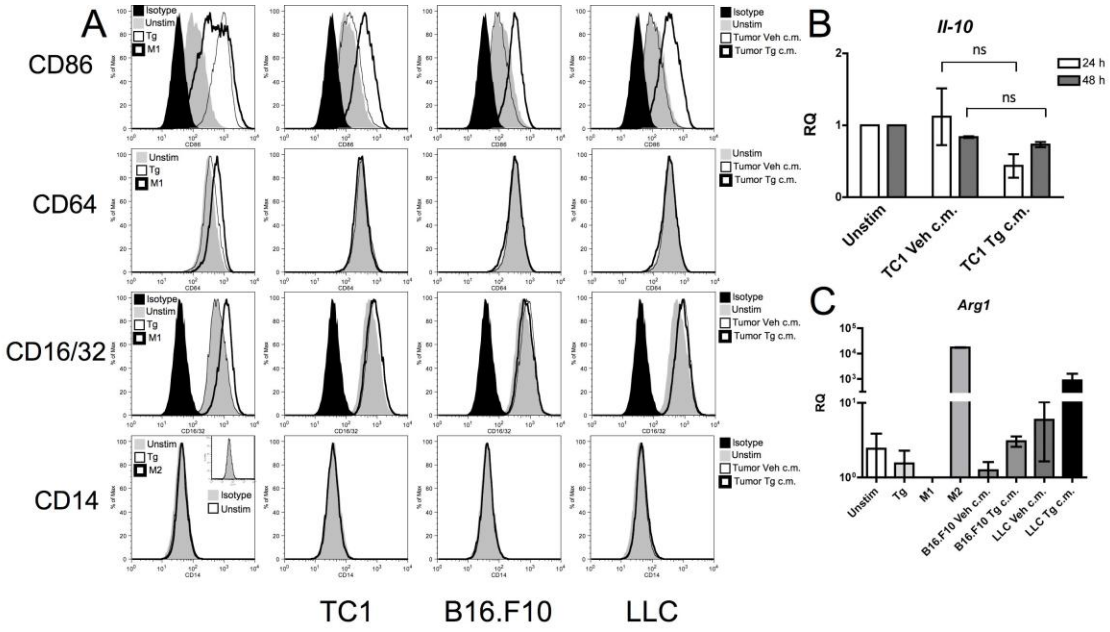

Figure 11. Conditioned medium from ER-stressed tumor cells polarizes macrophages toward an inflammatory/suppressive, tumor-associated macrophage phenotype. BMDM were cultured in conditioned medium of ER-stressed tumor cells (TC1, B16.F10, LLC Tg c.m.), control tumor cells (Veh c.m.), or culture medium with (Tg) or without (Unstim) Tg (300 nM) for 24 h. BMDM primed with IFN-γ (250 U/mL) and activated with LPS (100 ng/mL) (M1) or treated with IL-4 (50 ng/mL) (M2) served as controls. **(A)** Flow cytometry analysis of BMDM treated as indicated for macrophage cell surface phenotype markers. Results are of representative of three independent experiments. **(B)** *Il-10* transcription was quantified in BMDM treated for 24 or 48 h with conditioned medium of ER-stressed TC1 cells (TC1 Tg c.m.), control TC1 cells (TC1 Veh c.m.) by RT-qPCR. Columns indicate fold increase in transcript level (RQ) of each treatment group. The value of unstimulated controls was set arbitrarily to 1. Error bars represent SEM of two to three independent experiments. ns, Not significant ($P \geq 0.05$, unpaired, two-tailed *t* test). **(C)** Relative quantification of *Arg1* transcription of BMDM by RT-qPCR. Columns indicate fold increase in transcript level (RQ) of each treatment group. The value of an unstimulated control was set arbitrarily to 1. Error bars represent SEM of two biological replicates.

	M1	M^{TERS}	M2
CD80	+	+/-	-
CD86	+	+	-
CD16/32	+	-	-
CD64	+	-	-
CD14	-	-	+
IL-6	+	+	-
IL-23	+	+	-
Tnf-α	+	+	-
Il-10	-	-	+
Arg1	-	+	+

Figure 12. $TERS^{cm}$-imprinted BMDM (M^{TERS}) phenotype along the M1/M2 spectrum.

CHAPTER 2. Characterizing the sensors of TERS and pro-inflammation on BMDM.

Rationale

To delineate the mechanism by which transmission of ER stress and associated pro-inflammation may occur in "receiver" macrophages, we used BMDM from mice deficient in candidate receptors prospectively involved in tumor-myeloid cell communication and pro-inflammation: TLR2, IL-6R, and TLR4.

We reasoned that a role for TLR2 is plausible because TLR2 (*i*) is selectively upregulated under ER stress (81), (*ii*) is induced in dendritic cells and monocytes under hypoxic conditions (103), and (*iii*) mediates macrophage activation and IL-6 and TNF-α production in myeloid cells ligated by tumor cell-derived versican (97). IL-6R may be involved based on the fact that (*i*) both cancer cells and macrophages secrete IL-6, a proliferative anti-apoptotic pro-inflammatory cytokine, (*ii*) IL-6 production can be amplified by autocrine / paracrine mechanisms via IL-6 receptor (IL-6R) signaling (104), and (*iii*) the supernatant of serum-deprived LLC cells upregulates IL-6 production in myeloid cells (97). Finally TLR4 is a candidate as TLR4 signaling has been shown to synergize with UPR signaling (88, 89) and is involved in propagating inflammation in the tumor microenvironment (104).

Results

BMDM from TLR2 KO mice treated with TC1 ER stress-conditioned medium did not down-regulate either the ER stress or the proinflammatory cytokine responses

(Fig. 13A-B). Of note, we found that TLR2 KO BMDM secreted increased amounts of MIP-1α, MIP-1β, and monocyte chemoattractant protein-1 (MCP-1) in response to the TERS^{cm} relative to WT BMDM, suggesting that TLR2 may normally function as a negative regulator in response to proinflammatory stimuli (105, 106). As shown in Fig. 13A-B, IL-6R KO BMDM exposed to TERS^{cm} showed no decrease in the ER stress response and proinflammatory cytokine transcription compared with WT BMDM in response to TERS^{cm}. Collectively, these results argue that neither TLR2 nor IL-6R is involved in sensing transmissible ER stress.

In contrast, TLR4 KO BMDM treated with TC1 ER stress-conditioned medium showed decreased activation of the ER stress response and proinflammatory cytokine transcription compared with WT BMDM controls (Fig. 13A–C). In addition, TLR4 KO BMDM secreted lower amounts of MIP-1α and MIP-1β (53% and 61%, respectively) (Fig. 13D). Of note, this diminished effect was not due to an intrinsic defect in the ability of TLR4 KO BMDM to mount a UPR, as these cells respond to Tg treatment comparably to WT BMDM (Fig. 14).

We additionally probed the positive role of TLR4 agonism in TERS as it was recently demonstrated that, in macrophages, the ER stress response and TLR4 signaling synergize to cause IL-6 and IL-23 production at levels greater than those observed after either signaling event alone (88, 89). Thus, we reasoned that receiver macrophages undergoing transmissible ER stress would experience a more rapid or greater ER stress and proinflammatory cytokine response if concomitantly stimulated with LPS. TERS^{cm} from TC1 cells plus LPS (0.1 μg/mL) caused accelerated up-regulation of the ER stress response genes *Grp78*, *Gadd34*, and *Chop*, as well as proinflammatory cytokine genes,

which peaked at 6 h, compared with the ER stress conditioned medium alone (Fig. 15A), whose maximal effect on transcription occurs at 24 h (Fig. 10A). Likewise, macrophages secreted increased amounts of IL-6 and IL-23 (Fig. 15B). Thus, it appears that TLR4 may be involved both in sensing and potentiating transmissible ER stress in receiver macrophages.

Discussion

The phenomenon of transmissible ER stress described in these first two chapters (and Initial Studies) links tumor cells and macrophages in a new functional interplay that underscores the tumor cell's effort to seize control of myeloid cells in the tumor microenvironment, ostensibly leading to tumor growth and progression. We demonstrate that cancer cells under pharmacological or physiological ER stress (transmitters) can condition macrophages (receivers) to mirror the behavior of cancer cells (i.e., ER stress and transcriptional up-regulation of a tumorigenic, proinflammatory response). Instructive models in biological systems such as "quorum sensing" in bacteria (107) and "infectious" transplantation tolerance in mice (108), both of which have effects on gene expression and cell regulation via wireless cell-to-cell communication, constitute precedents to our observation. Further support is provided by the observation that tumor cells under ER stress can secrete Par-4, which induces an ER stress response in neighboring tumor cells upon binding to surface Grp78 (109). Further, there is evidence that cell surface Grp78 is a promiscuous binder of many molecules and can mediate a downstream UPR upon ligation (110, 111).

Of note, we found that the transmissible factor(s) released by ER-stressed tumor cells is sensed by TLR4 and is also amplified through concomitant TLR4 signaling by LPS. This suggests that endogenous TLR4 ligands (oxidized phospholipids, tenascin-C, β-defensin, heat shock proteins, etc. (112)) or infection by Gram-negative bacteria, could be cofactors in the tumorigenic effects of ER stress-initiated inflammation in the tumor microenvironment.

That transmissible ER stress conditions macrophages to a proinflammatory phenotype is relevant to a better understanding of the tumor–microenvironment interplay, and adds further complexity to the apparent paradox on the coexistence of proinflammation and anti-inflammation in the tumor microenvironment, which includes myeloid cells recruited to the tumor site that are believed to be prevalently anti-inflammatory/suppressive cells (113). However, as discussed earlier, tumor-associated macrophages can secrete inflammatory factors such as cytokines, chemokines, and metalloproteinases that promote tumorigenesis (6), and can be polarized by inflammatory mediators to a suppressive phenotype (65). Interestingly, while $TERS^{cm}$-polarized BMDM do produce inflammatory cytokines, especially with synergistic TLR4 agonism, they also up-regulate arginase transcription, suggesting a mixed pro-inflammatory/suppressive phenotype, a myeloid phenotype increasingly observed in the tumor microenvironment (77, 114).

Chapter 2, in part, has been published in the manuscript: Mahadevan, N.R., Rodvold, J., Sepulveda, H., Rossi, S., Drew, A., and Zanetti, M. Transmission of ER stress and pro-inflammation from tumor cells to myeloid cells. *Proc Natl Acad Sci USA*,

108(16):6561-6, 2011. The dissertation author was the primary investigator and author of this paper and the other authors helped perform the research and write the manuscript.

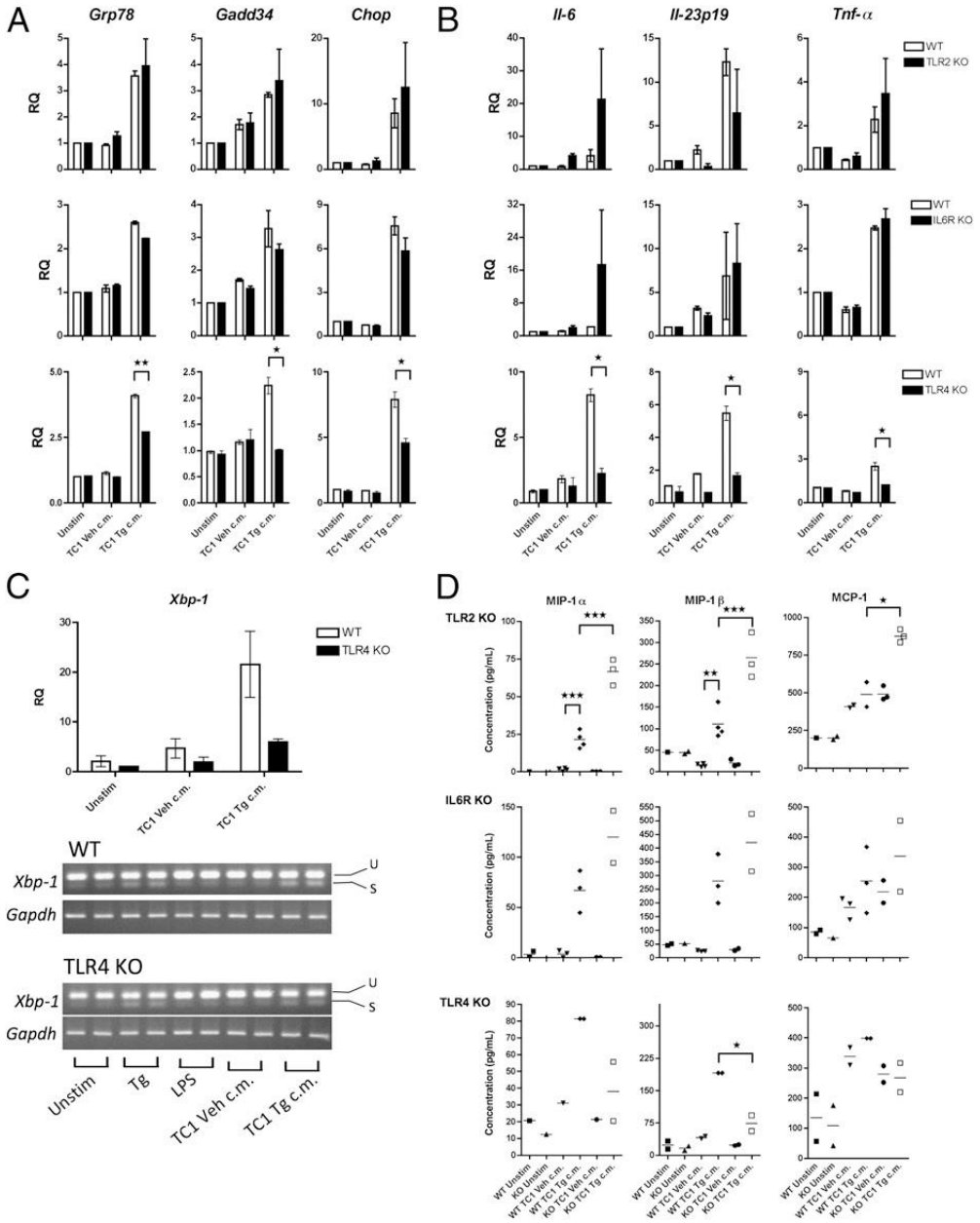

Figure 13. TLR4 senses transmissible ER stress, whereas TLR2 and IL6R do not. BMDM generated from WT (WT) C57BL/6 mice, TLR2 KO mice, IL6RKO, or TLR4 KO mice were cultured in ER-stressed conditioned medium from TC1 cells (TC1 Tg c.m.), control TC1 cells (TC1 Veh c.m.), or culture medium with or without (Unstim) LPS for 24 h. RNA was isolated from macrophages and analyzed by RT-qPCR for **(A)** UPR activation and **(B)** proinflammatory cytokine gene transcription. Columns indicate fold increase in transcript level (RQ) of each treatment group. For each genotype, the value of an unstimulated control was set arbitrarily to 1. Error bars represent SEM of two to four biological replicates. $*P < 0.05$, $**P < 0.01$, $***P < 0.001$, unpaired, two-tailed *t* test. **(C)** Xbp-1 activation and splicing. u, Unspliced; s, spliced. **(D)** BMDM supernatants were tested for presence of chemokines using the Multiplex cytometric bead assay. $*P < 0.05$, $**P < 0.01$, $***P < 0.001$, unpaired, two-tailed *t* test.

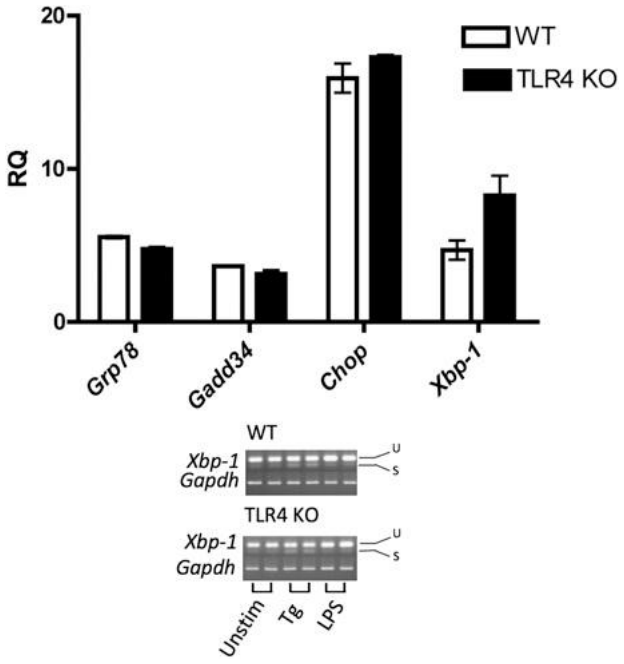

Figure 14. TLR4 KO BMDM mount UPR comparable to WT BMDM. TLR4 KO and WT BMDM were treated with Tg (300 nM) for 24 h. RNA was isolated and analyzed by RT-qPCR for UPR activation and proinflammatory cytokine gene transcription. Columns indicate fold increase in transcript level (RQ) of each treatment group. The value of an unstimulated control was set arbitrarily to 1. Error bars represent SEM of two biological replicates. Values for WT and KO gene expression were not statistically different. $P \geq 0.05$, unpaired, two-tailed *t* test. u, unspliced; s, spliced.

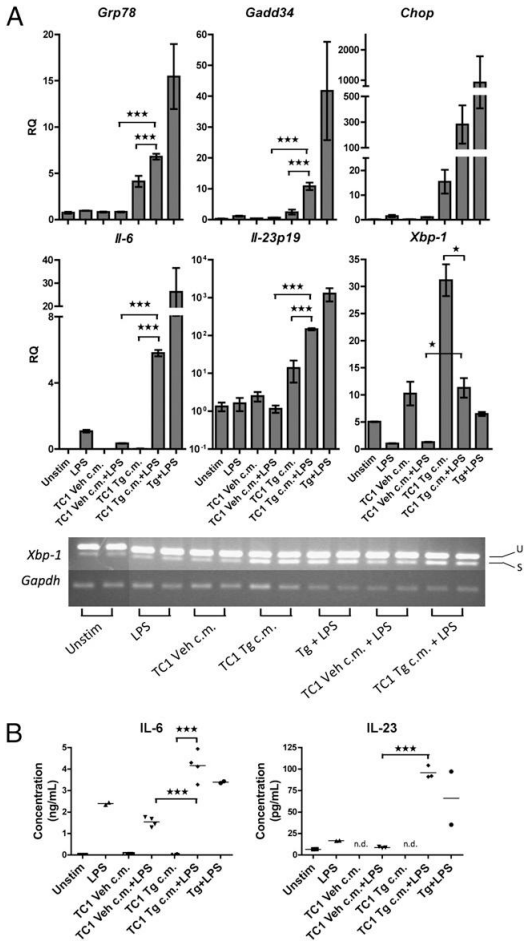

Figure 15. TLR4 signaling potentiates the effect of transmissible ER stress on macrophages. Macrophages were cultured in either conditioned medium of ER-stressed TC1 cells (TC1 Tg c.m.) or control TC1 cells (TC1 Veh c.m.), with or without LPS (100 ng/mL), culture medium containing LPS or thapsigargin (Tg, 300 nM), or culture medium alone (Unstim) for 6 h. Macrophages cultured in medium containing Tg (300 nM) plus LPS serve as a positive control. **(A)** RNA was isolated from macrophages and analyzed by RT-qPCR for UPR activation and proinflammatory cytokine gene transcription. Columns indicate fold increase in transcript level (RQ) of each treatment group. LPS-treated control was set arbitrarily to 1. Error bars represent SEM of two to four biological replicates. *$P < 0.05$, ***$P < 0.001$, unpaired, two-tailed *t* test. u, Unspliced; s, spliced. **(B)** Supernatants from macrophages in A were analyzed by multiplex cytometric bead array for presence of IL-6 and IL-23. n.d., Not detectable. ***$P < 0.001$, unpaired, two-tailed *t* test.

CHAPTER 3. Determining the phenotype of bone marrow derived dendritic cells (BMDC) exposed to $TERS^{cm}$

Rationale

Solid tumors are infiltrated by host immune cells, including cells of myeloid origin such as macrophages and dendritic cells (DC), which serve as a link between innate and adaptive immunity. Under the influence of tumor-derived signals, these cells reportedly polarize to a phenotype that facilitates tumor growth through both inefficient priming of anti-tumor T cell responses and T cell-independent mechanisms such as promotion of angiogenesis and release of tumorigenic cytokines (65). Tumor-infiltrating dendritic cells have been shown to be present in tumors of several histological origins (e.g. melanocyte (73), lung (74), breast (75)) and facilitate tumor growth by inhibiting anti-tumor $CD8^+$ T cell function and perhaps by direct promotion of tumor growth and angiogenesis (75). Moreover, although equipped with signals necessary for efficient T cell priming, i.e., MHC Class I and costimulatory molecules, tumor-infiltrating DC instead inhibit T cell proliferation and induce T cell anergy due to inadequate peptide presentation and increased arginase activity (74, 75). However, the nature of the tumor-derived signals driving myeloid DC dysregulation, which ultimately affects the establishment of anti-tumor CD8+ T cell immunity, has yet to be elucidated. Unquestionably, identifying tumor-imparted signals that subvert anti-tumor immunity would represent a crucial new step in understanding the relationship between tumors and immunity.

Although discovered in macrophages, we reasoned that BMDC could be the target of tumor UPR-borne cell-extrinsic effects, dysregulating their function, and ultimately facilitating tumor escape and growth. In chapters 3 and 4, we extend our original findings on $TERS^{cm}$-imprinted BMDM by examining the transcriptional and functional consequences of TERS on BMDC, hypothesizing that $TERS^{cm}$-activated BMDC may resemble TIDC phenotypically and functionally.

Results

First, the cell-extrinsic effects of tumor UPR were assessed by culturing bone marrow-derived dendritic cells (BMDC) in the conditioned medium (c.m.) from ER-stressed murine tumor cells (prostate, TRAMP-C1 [TC1]; melanoma, B16.F10; and Lewis lung carcinoma, LLC). Under these conditions, BMDC mounted a global ER stress response, as evinced by the transcriptional upregulation of *Grp78*, and two downstream UPR effector molecules, *Xbp-1s*, and *Chop* (Fig. 16A), of the IRE1α and PERK pathways, respectively. $TERS^{cm}$-imprinted BMDC also upregulated the transcription of the pro-inflammatory, pro-tumorigenic cytokines, *Il-6*, *Il-23p19*, and, in two of the three cell lines tested, *Tnf-a* (Fig. 16A). Congruently, we detected increased secretion of IL-6, IL-23, TNF-α, and in addition the chemokines/cytokines MIP-1α, MIP-1β, MCP-1, and IL-1β (Fig. 16B). We did not detect IL-10 (Fig. 16C). Importantly, $TERS^{cm}$-imprinted BMDC also upregulated transcription of *Arg1* (Fig. 16A), which codes for arginase, a known suppressor of T cell function (115). Taken together, these findings suggest that, similar to macrophages (116), BMDC are a susceptible target of TERS, through which they assume a pro-inflammatory/suppressive phenotype.

Within 24 h of culture in TERS^{cm}, BMDC changed morphology, acquiring characteristics of activated, mature DC, including increased cell size and the development of elongated dendrites (Fig. 17). We confirmed that TERS-imprinted BMDC undergo activation and maturation, as they upregulate expression of MHC Class I and Class II, and the costimulatory molecules, CD86, CD80, and, to a lesser extent, CD40 (Fig. 18). These cells were CD8α^- (Fig. 19), confirming their myeloid origin. GR-1, which is expressed at low levels in immature BMDC, was not upregulated by exposure to TERS^{cm} (Fig. 19). This distinguishes the phenotype of TERS^{cm}-imprinted BMDC from that of myeloid-derived suppressor cells, a class of myeloid cells that accumulate in the tumor microenvironment, where they suppress anti-tumor T cell immunity (70, 75). Additionally, TERS^{cm}-imprinted BMDC only slightly increased PDL-1 expression above constitutive levels (Fig. 19).

Chapter 3, in part, has been submitted to *Science* under the title, "Cell-extrinsic effects of tumor ER stress imprint myeloid dendritic cells and impair CD8$^+$ T cell priming," authored by, Navin R. Mahadevan, Veronika Anufreichik, Jeffrey Rodvold, Homero Sepulveda, and Maurizio Zanetti. The dissertation author was the primary investigator and author of this paper and the other authors helped perform the research and write the manuscript.

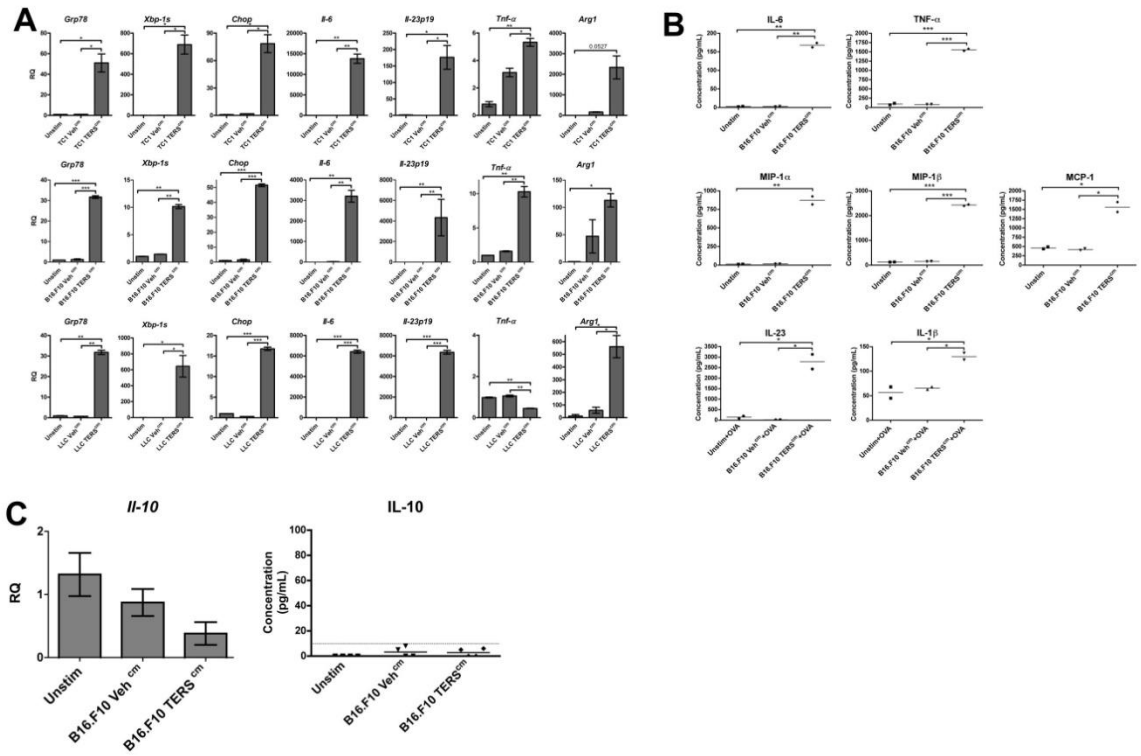

Figure 16. TERS^{cm}-imprinted BMDC upregulate UPR elements and produce pro-inflammatory cytokines. BMDC were cultured for 24 h in TERS^{cm} or Veh^{cm} from the tumor cell lines indicated, or media alone (Unstim). **(A)** RNA was isolated from BMDC and analyzed by RT-qPCR for UPR activation and proinflammatory cytokine gene transcription. Columns indicate fold increase in transcript level (RQ) of each treatment group. An Unstim control was set arbitrarily to 1. Error bars represent SEM of two biological replicates and are representative of six independent experiments. *$P < 0.05$, **$P < 0.01$, ***$P < 0.001$, unpaired, two-tailed *t* test. **(B)** Supernatants from BMDC in (A) were analyzed by cytometric bead array for presence of the cytokines indicated. . *$P < 0.05$, **$P < 0.01$, ***$P < 0.001$, unpaired, two-tailed *t* test. **(C)** RNA was isolated from BMDC and analyzed by RT-qPCR for *Il-10* transcription. Columns indicate fold increase in transcript level (RQ) of each treatment group. An Unstim control was set arbitrarily to 1. Error bars represent SEM of four biological replicates pooled from two independent experiments. BMDC supernatants were interrogated for IL-10; dotted line indicates threshold of detection.

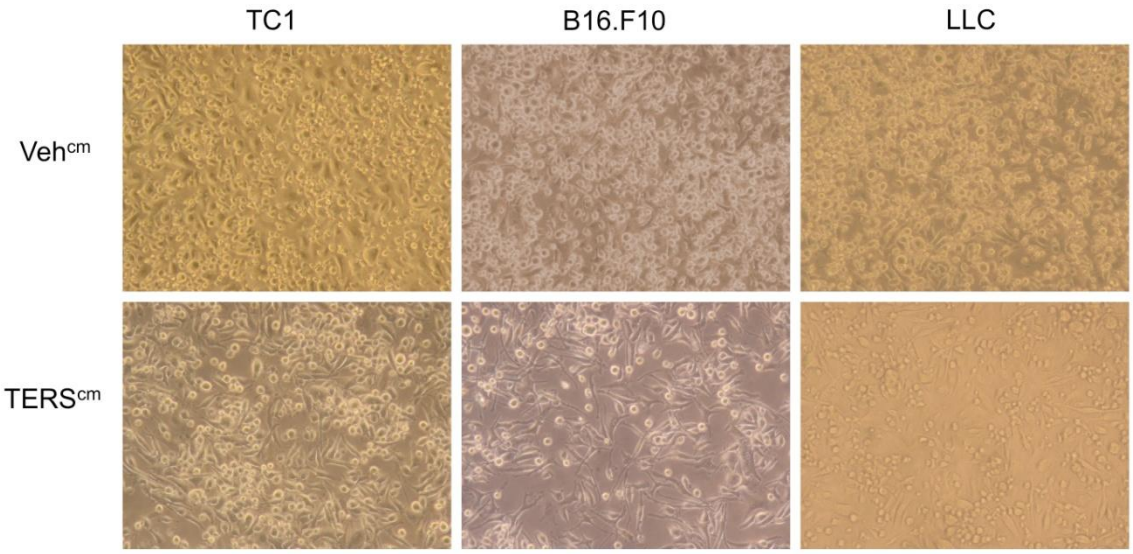

Figure 17. TERS^{cm}-imprinted BMDC exhibit an activated, mature morphology. BMDC were cultured for 24 h in TERS^{cm} or Veh^{cm} from the tumor cell lines indicated and photographed under 20X objective. Results are representative of at least three independent experiments.

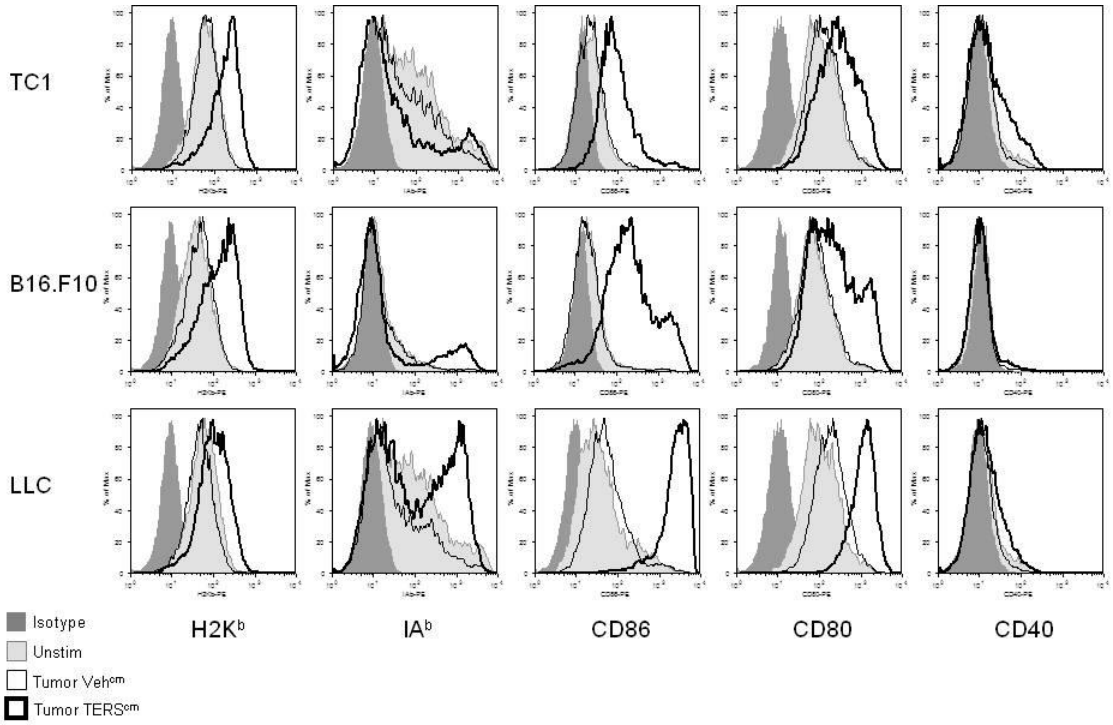

Figure 18. TERS^{cm}-imprinted BMDC polarize to an activated, mature immunophenotype. BMDC were cultured for 24 h in TERS^{cm} or Veh^{cm} from the tumor cell lines indicated, or media alone (Unstim), and interrogated for the cell surface markers indicated by flow cytometry. Results are representative of at least three independent experiments.

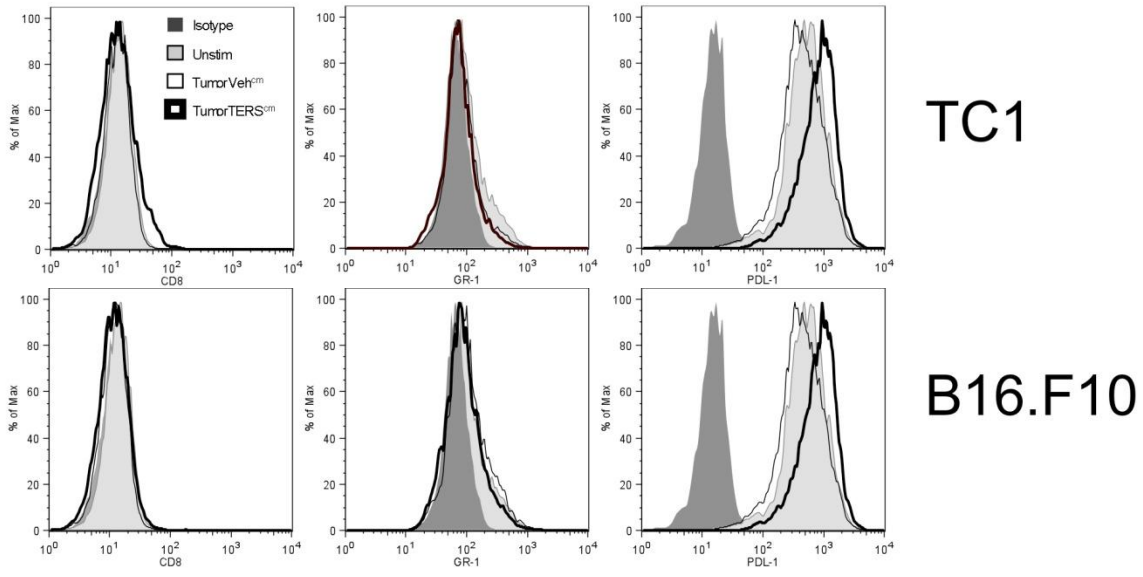

Figure 19. TERS^{cm}-imprinted BMDC are myeloid cells distinct from MDSC. BMDC were cultured for 24 h in TERS^{cm} or Veh^{cm} from the tumor cell lines indicated, or media alone (Unstim), and interrogated for the cell surface markers indicated by flow cytometry. Results are representative of three independent experiments.

CHAPTER 4. Examining cross-presentation by TERS^{cm}-imprinted BMDC, and subsequent CD8^{+} T cell activation

Rationale

We have shown that tumor cells under ER stress can influence BMDM and BMDC to undergo ER stress and polarize them to release tumorigenic, pro-inflammatory cytokines, suggesting a T cell-independent mechanism of promoting tumor growth. However, as BMDC are also powerful regulators of cellular immunity, it is prudent to examine the effect of TERS^{cm} on the antigen presentation and T cell priming ability of BMDC. We focused on cross-presentation, a mode of exogenous antigen presentation on MHC Class I, as this is likely how exogenous tumor antigens are presented to T cells in the tumor microenvironment. We examined the activation of transgenic, antigen-specific CD8^{+} T cells in response to TERS^{cm}-imprinted myeloid cell cross presentation, as CD8^{+} T cells have been shown to be mainly responsible for immune rejection of tumors.

Results

To this end, we used soluble ovalbumin (OVA) as a model exogenous antigen and the monoclonal antibody, 25.D1.16, to specifically recognize the MHC Class I-restricted OVA 257-264 SIINFEKL peptide bound to the H2-K^{b} molecule on BMDC (Fig. 20A). We found that TERS^{cm}-imprinted BMDC display a reduced capacity to cross-present the SIINFEKL peptide as compared to control BMDC (Fig. 20B), notwithstanding the fact that the surface expression of MHC Class I molecules remained similar to or actually increased over that of untreated OVA-fed BMDC (Fig. 21).

We then investigated the ability of TERS^{cm}-imprinted BMDC to cross-prime naïve CD8^{+} T cells from transgenic OT-I mice, whose TCR recognizes SIINFEKL/H2-K^{b} complex, in an *in vitro* co-culture assay. When provided with exogenous OVA, control unstimulated BMDC or BMDC treated with conditioned medium from unstressed tumor cells (Veh^{cm}) efficiently induced antigen-specific OT-I T cell activation and proliferation, as demonstrated by conversion to an activated CD69^{+}/CD25^{+}/CD62L^{lo}/CD44^{+} phenotype (Fig. 22A) and by 5-(and-6)-Carboxyfluorescein Diacetate, Succinimidyl Ester (CFDA-SE) dilution (Fig. 22B), respectively. In contrast, OT-I CD8^{+} T cells co-cultured with OVA-fed, TERS^{cm}-imprinted BMDC, while activated, proliferated poorly, resulting in a decreased percentage of activated, dividing T cells (Fig. 22B), suggestive of a proliferation-refractory status. As expected, coculture of OT-I T cells with untreated or TERS^{cm}-imprinted BMDC without antigen did not result in activation or proliferation (Fig 22A and Fig. 23). The proliferation defect was not associated with PD-1 upregulation on T cells (Fig. 24). Addition of excess exogenous antigen (1 μg/mL) rescued T cell proliferation only at a high dose (Fig. 25A and Fig. 26). Because a proliferation-refractory phenotype could reflect T cell anergy a defect that can be rescued by exogenous IL-2 as shown in CD4^{+} T cells (117), we interrogated the effect of exogenous administration of this cytokine during initial cross-priming and subsequent restimulation by antigen. Exogenous administration of IL-2 during cross-priming failed to rescue OT-I T cell proliferation (Fig. 25B). Restimulation with antigen again underscored a proliferative defect that could not be corrected with exogenous IL-2 (Fig. 25B). Thus, we argue that proliferation-refractory CD8^{+} T cells arising from interaction with TERS^{cm}-imprinted BMDC does not fulfill the classical criteria of anergy.

We reasoned that the proliferative defect of OT-I T cells co-cultured with TERS^{cm}-imprinted BMDC could be that of T cells that have undergone cell cycle arrest due to arginine deprivation (75). Indeed, we detected a significant population of OT-I cells in G0 after cross-priming by TERS^{cm}-imprinted BMDC (Fig. 27). Because TERS^{cm} upregulates arginase (*Arg1*) expression in BMDC, we probed the contribution of this metabolic pathway to the T cell priming defect. The addition of exogenous L-arginine to the co-culture medium did not improve T cell proliferation. In contrast, the addition of L-norvaline, an arginine analogue and competitive inhibitor of arginase, rescued in great part (80 %) T cell proliferation (Fig. 25C). Taken together, these results suggest that downstream effects of tumor UPR-mediated arginase activity in BMDC contribute to the inhibition of proliferation of T cells. Based on the fact that TERS^{cm}-imprinted BMDC can also inhibit T cell proliferation in this antigen-independent manner, we further hypothesized that TERS^{cm}-imprinted BMDC could exert a dominant suppressive effect on the ability of normal BMDC to cross-prime CD8$^+$ T cells. When TERS^{cm}-imprinted BMDC, with or without antigen, were added to cocultures of OT-I T cells and normal BMDC or BMDC previously cultured in unstressed tumor cell supernatant, antigen-specific T cell proliferation was again suppressed (Fig. 25D). Surprisingly, the addition of L-norvaline to these cocultures did not significantly rescue T cell proliferation (Fig. 28). Thus, TERS^{cm}-imprinted BMDC can suppress the T cell cross-priming capacity of normal BMDC in an antigen-independent, arginase-independent manner.

To initially characterize the lineage of T cells cross-primed by TERS^{cm}-imprinted BMDC, we measured the expression of genes relevant to T cell fate determination by RT-qPCR and cytokine secretion using a multiplex cytometric assay. Regulatory CD8$^+$ T

cells have been isolated from human tumors and have been found to secrete IL-10, TNF-α, and IFN-γ, express FOXP3 and low levels of the costimulatory molecule CD28, and suppress the proliferation of $CD8^+$ effector T cells (118, 119). $CD8^+$ T cells cross-primed by $TERS^{cm}$-imprinted BMDC showed transcriptional upregulation of the cytokines, *Il-10* and *Tnf-α* (Fig. 25E). The transcriptional upregulation of *Foxp3* and downregulation of the costimulatory molecule CD28 (Fig. 25E and F) was also observed, suggesting that these cells may be undergoing plastic differentiation to a T regulatory cell phenotype. OT-I cells cross-primed by $TERS^{cm}$-imprinted BMDC did not increase the transcription of *Il-17a* (Fig, 25E). Surprisingly, these T cells also demonstrated dramatic splicing of *Xbp-1* with only marginal upregulation of other elements of the UPR signaling pathways (Fig. 25E). Further investigation is required to elucidate the role, if any, of XBP-1s in the proliferation of $CD8^+$ T cells and their cell fate.

Chapter 4, in part, has been submitted to *Science* under the title, "Cell-extrinsic effects of tumor ER stress imprint myeloid dendritic cells and impair $CD8^+$ T cell priming," authored by, Navin R. Mahadevan, Veronika Anufreichik, Jeffrey Rodvold, Homero Sepulveda, and Maurizio Zanetti. The dissertation author was the primary investigator and author of this paper and the other authors helped perform the research and write the manuscript.

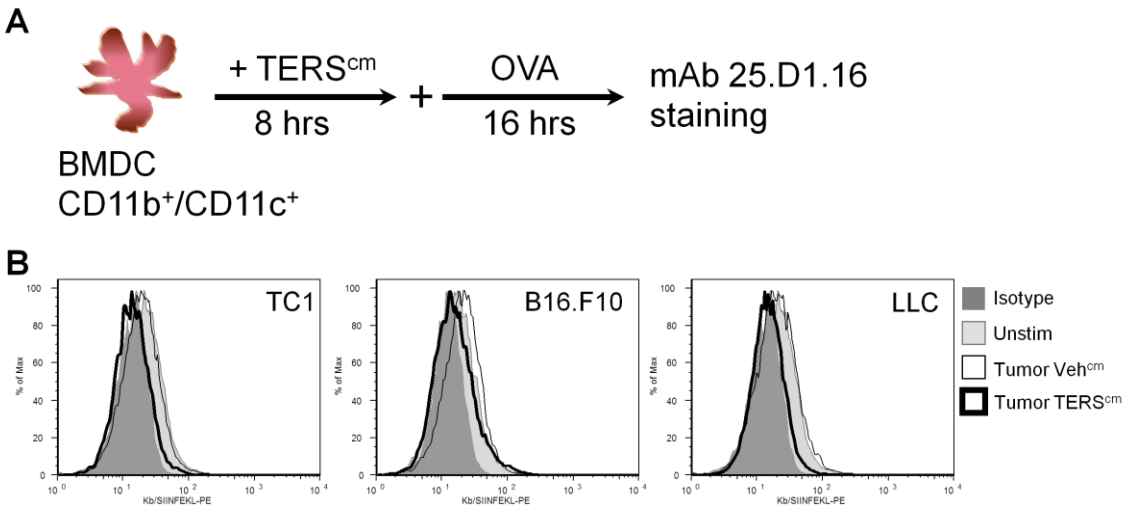

Figure 20. TERS^{cm}-imprinted BMDC do not efficiently cross-present exogenous antigen. (A) BMDC were cultured in TERS^{cm} or Veh^{cm} from the tumor cell lines indicated, or media alone (Unstim) for 8 hours after which ovalbumin (1 mg/mL) was added directly to cultures for a further 16 h. **(B)** BMDC presentation of the SIINFEKL/H2-Kb complex was monitored using the 25.D1.16 antibody using flow cytometry. Results are representative of three independent experiments.

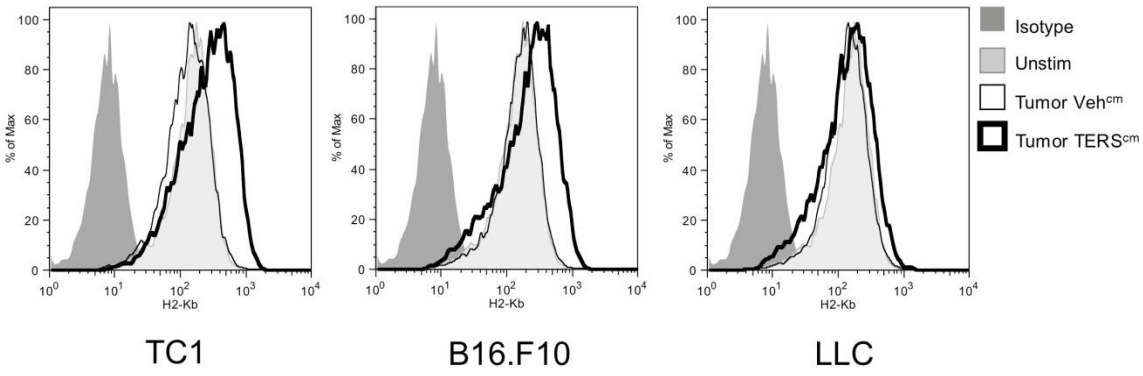

Figure 21. Ovalbumin-fed TERS^{cm}-imprinted BMDC do not decrease global MHC Class I molecule expression. BMDC were cultured in TERS^{cm} or Veh^{cm} from the tumor cell lines indicated, or media alone (Unstim) for 8 hours after which ovalbumin (1 mg/mL) was added directly to cultures for a further 16 h. H2-K^{b} expression was then measured by flow cytometry. Results are representative of four independent experiments.

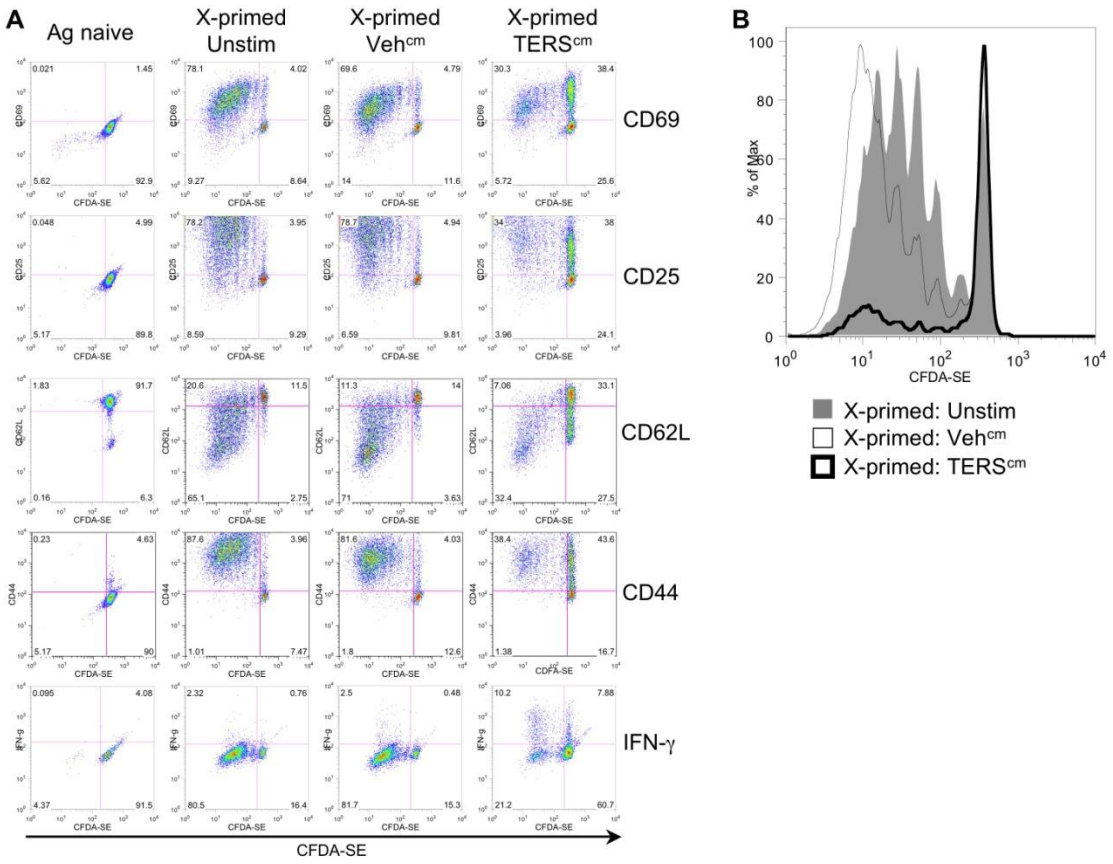

Figure 22. CD8$^+$ T cells cross-primed by TERS^{cm}-imprinted BMDC become activated but do not proliferate. BMDC were cultured in TERS^{cm} or Veh^{cm} from B16.F10 tumor cells, or media alone (Unstim) for 8 hours after which ovalbumin (1 mg/mL) was added directly to cultures for a further 16 h. Unstim BMDC not fed OVA (Ag naïve) were used as a control. BMDC were co-cultured with CFDA-SE-labeled CD8$^+$ OT-I transgenic T cells. After 96 h co-culture, CD8$^+$ T cells were interrogated for **(A)** expression of the activation markers indicated and **(B)** proliferation (CFDA-SE dilution) by flow cytometry. Results are representative of eight independent experiments.

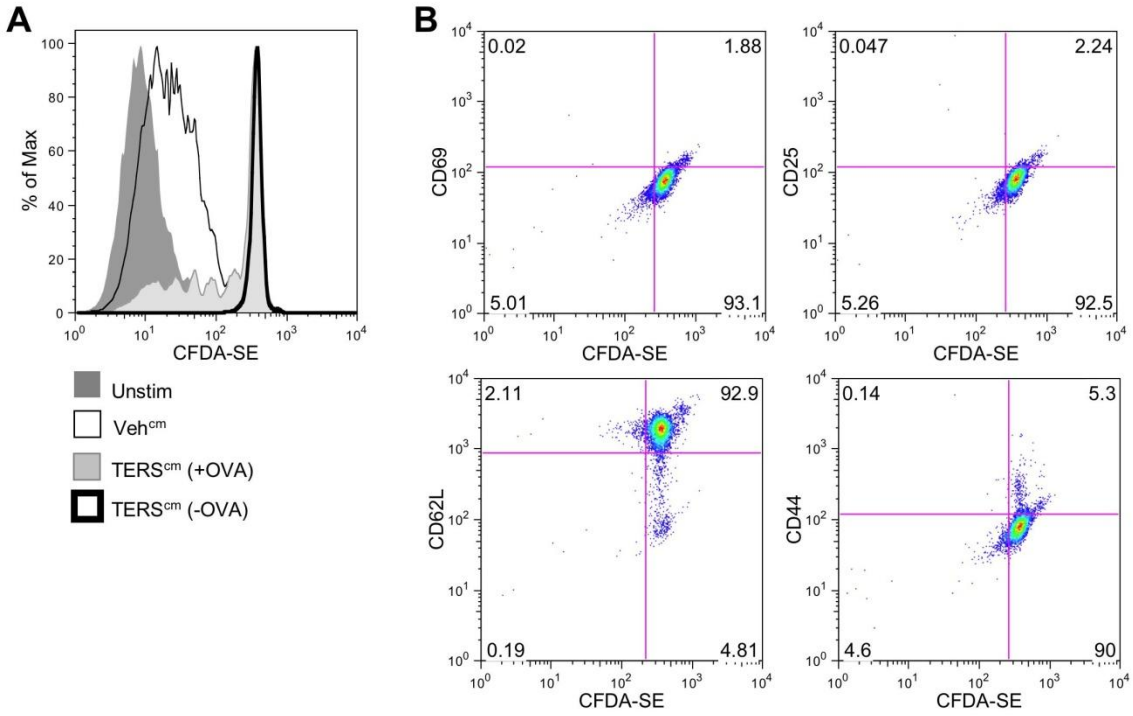

Figure 23. CD8$^+$ T cells cross-primed by TERS^{cm}-imprinted BMDC without antigen do not proliferate or become activated. BMDC were cultured in TERS^{cm} or Veh^{cm} from B16.F10 tumor cells, or media alone (Unstim) for 8 hours after which ovalbumin (1 mg/mL) was (+OVA) or was not (-OVA) added directly to cultures for a further 16 h. BMDC were then co-cultured with CFDA-SE-labeled CD8$^+$ OT-I transgenic T cells. After 96 h co-culture, CD8$^+$ T cells were interrogated for **(A)** proliferation (CFDA-SE dilution) and **(B)** expression of the indicated activation markers, by flow cytometry. Results are representative of two experiments.

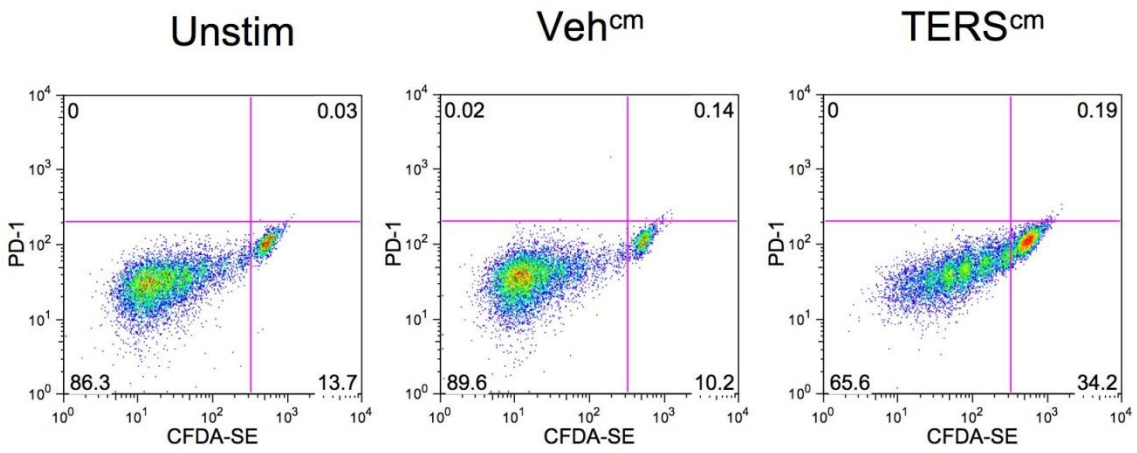

Figure 24. CD8+ T cells cross-primed by TERS^{cm}-imprinted BMDC do not upregulate PD-1 expression. BMDC were cultured in TERS^{cm} or Veh^{cm} from B16.F10 tumor cells, or media alone (Unstim) for 8 hours after which ovalbumin (1 mg/mL) was added directly to cultures for a further 16 h. BMDC were then co-cultured with CFDA-SE-labeled CD8^{+} OT-I transgenic T cells. After 96 h co-culture, CD8^{+} T cells were interrogated for CFDA-SE dilution and PD-1 expression by flow cytometry. Results are representative of three experiments.

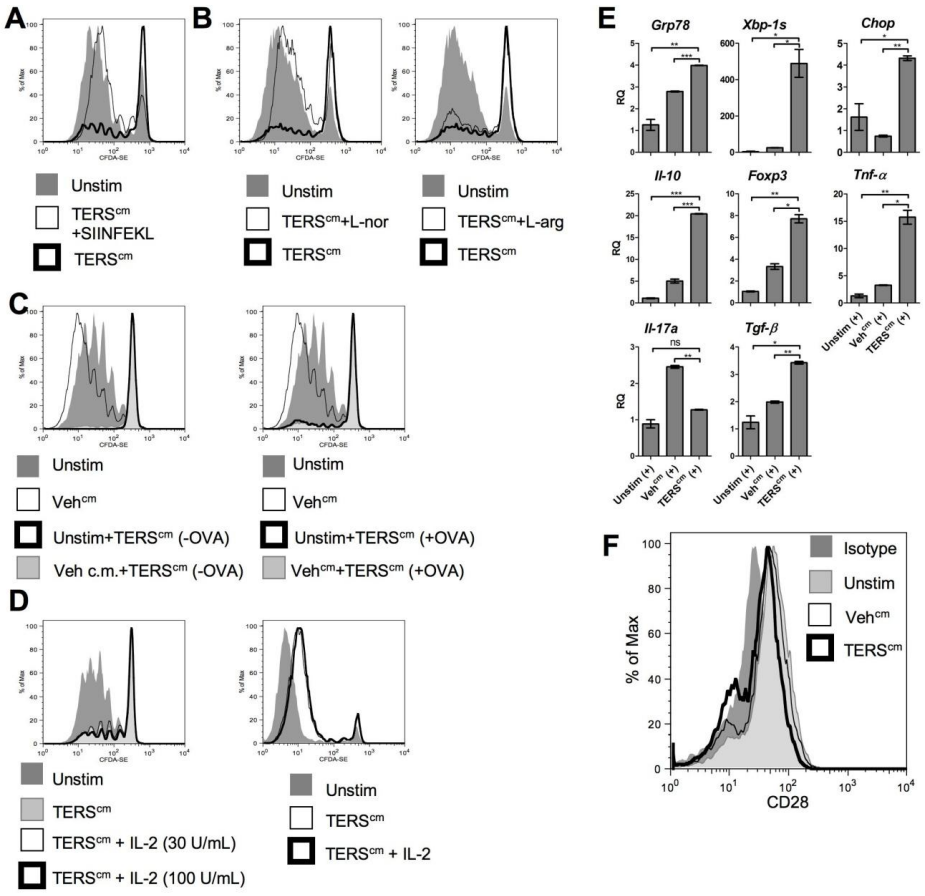

Figure 25. CD8$^+$ T cells cross-primed TERS^{cm}-imprinted BMDC display an arginase-dependent proliferation-refractory phenotype and are regulatory/suppressive. BMDC were cultured in TERS^{cm} or Veh^{cm} from B16.F10 tumor cells, or media alone (Unstim) for 8 hours after which ovalbumin (1 mg/mL) was (+OVA) or was not (-OVA) added directly to cultures for a further 16 h. BMDC were then co-cultured with CFDA-SE-labeled or unlabeled CD8$^+$ OT-I transgenic T cells for 96 h. **(A)** CD8$^+$ OT-I T cells were additionally co-cultured with SIINFEKL-pulsed TERS^{cm}-imprinted BMDC and CD8$^+$ T cell proliferation was measured by CFDA-SE dilution. Results are representative of three independent experiments. **(B)** L-norvaline (L-nor, 10 mM) or L-arginine (L-arg, 2 mM) was added to the indicated co-cultures and CD8$^+$ T cell proliferation was measured by CFDA-SE dilution. Results are representative of three independent experiments. **(C)** BMDC with(+) and without (-) OVA were cocultured with CFDA-SE-labeled CD8$^+$ OT-I T cells at a 1:1:2.5 ratio as above and T cell proliferation was measured by CFDA-SE dilution. Results are representative of three independent experiments. **(D)** (*left panel*) Recombinant mouse IL-2 was added at the indicated concentrations to the indicated co-cultures and CD8$^+$ T cell proliferation was measured by CFDA-SE dilution. Results are representative of two independent experiments. (*right panel*) After 4-day co-culture, CFDA-SE-labeled T cells were isolated and rested for 2 days before restimulation with SIINFEKL-pulsed BMDC in the presence or not of recombinant mouse IL-2 (30 U/mL). CD8$^+$ T cell proliferation was measured by CFDA-SE dilution. Results are representative of two independent experiments. **(E)** After 96 h co-culture, CFDA-SE-labeled T cells were purified. RNA was isolated and analyzed by RT-qPCR for transcription levels of the indicated genes. Columns indicate fold increase in transcript level (RQ) of each treatment group. An Unstim (+) control was set arbitrarily to 1. Error bars represent SEM of two biological replicates and are representative of four independent experiments. *P < 0.05, **P < 0.01, ***P < 0.001, ns = not significant, unpaired, two-tailed t test. **(F)** After 4-day coculture with the indicated BMDC populations, unlabeled CD8$^+$ T cells were interrogated for CD28 expression by flow cytometry. Results are representative of two independent experiments.

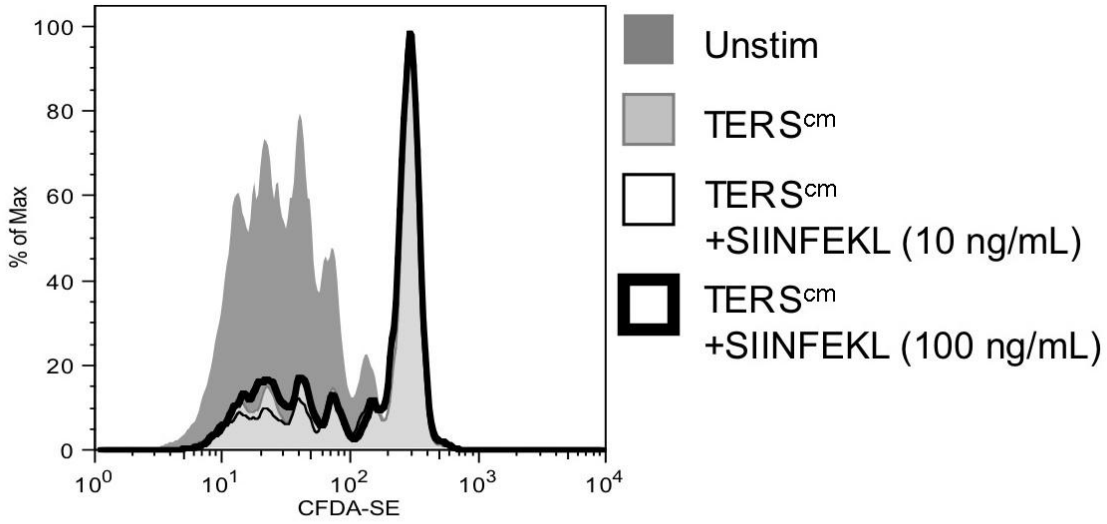

Figure 26. Moderate amounts of exogenous antigen do not rescue proliferation of CD8$^+$ T cell cross-primed by TERS^{cm}-imprinted BMDC. BMDC were cultured in TERS^{cm} from B16.F10 tumor cells for 8 hours after which ovalbumin (1 mg/mL) was added directly to cultures for a further 16 h. BMDC were then pulsed with the indicated concentrations of the SIINFEKL peptide for 4 h and co-cultured with CFDA-SE-labeled CD8$^+$ OT-I transgenic T cells. After 96 h co-culture, CD8$^+$ T cells were interrogated for proliferation (CFDA-SE dilution) by flow cytometry. Results are representative of two independent experiments.

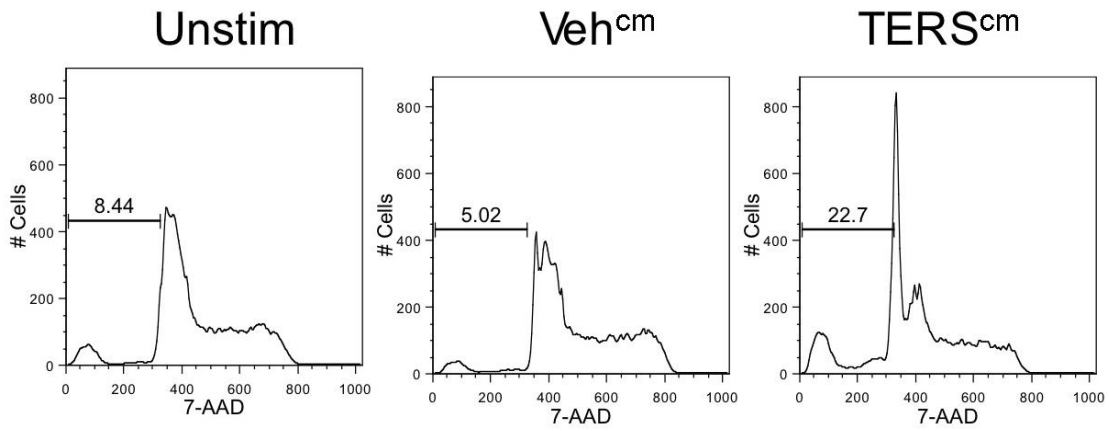

Figure 27. CD8$^+$ T cells cross-primed by TERS^{cm}-imprinted BMDC undergo cell cycle arrest. BMDC were cultured in TERS^{cm} or Veh^{cm} from B16.F10 tumor cells, or media alone (Unstim) for 8 hours after which ovalbumin (1 mg/mL) was (+OVA) or was not (-OVA) added directly to cultures for a further 16 h. BMDC were then co-cultured with CFDA-SE-labeled CD8$^+$ OT-I transgenic T cells.. After 96 h co-culture, T cell cycle status was interrogated using 7-AAD staining as determined by flow cytometry. Results are representative of two independent experiments.

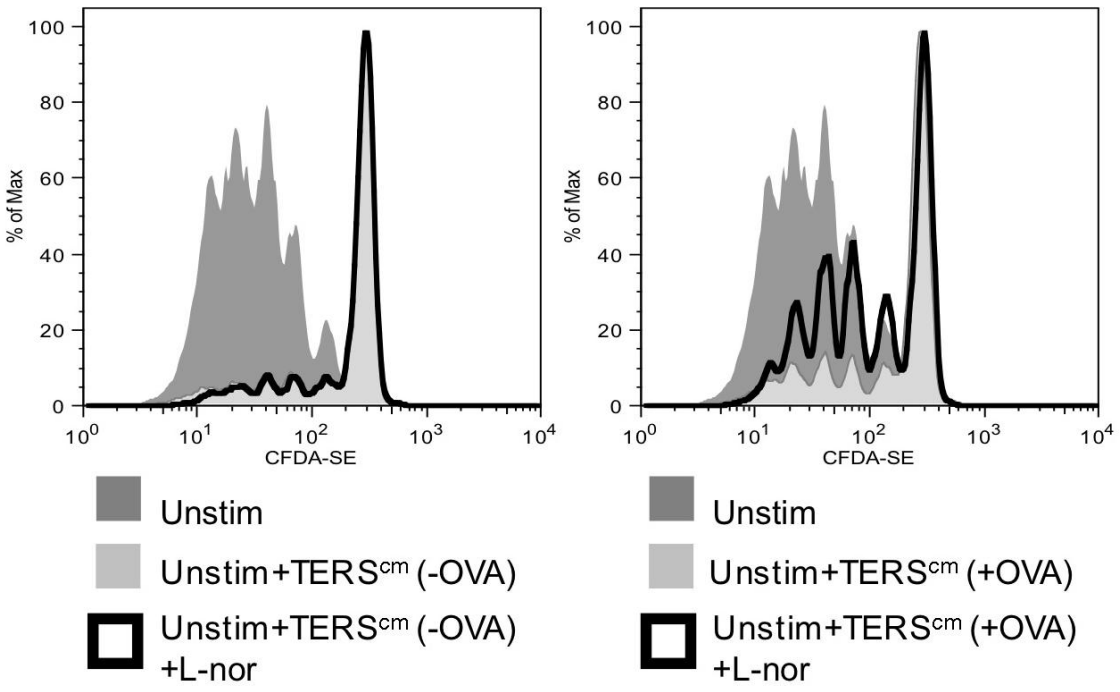

Figure 28. The dominant suppressive activity of TERS^{cm}-imprinted BMDC is not responsive to arginase inhibition. BMDC were cultured in TERS^{cm} or Veh^{cm} from B16.F10 tumor cells, or media alone (Unstim) for 8 hours after which ovalbumin (1 mg/mL) was (+OVA) or was not (-OVA) added directly to cultures for a further 16 h. OVA-fed Unstim BMDC were cocultured with TERS^{cm}-imprinted BMDC with or without antigen and CFDA-SE-labeled CD8$^+$ OT-I transgenic T cells in the presence or not of L-norvaline (L-nor, 10 mM). After 96 h co-culture, CD8$^+$ T cells were interrogated for proliferation (CFDA-SE dilution) by flow cytometry. Results are representative of two independent experiments.

CHAPTER 5. Investigating the functional role of TERS^{cm}-imprinted BMDC in the facilitation of tumor growth *in vivo*.

Rationale

In the previous four chapters, we have established that the tumor ER stress response can, in a cell-extrinsic manner, influence myeloid cells by modulating their T cell-independent and –dependent functions. We hypothesized that defective $^{CD8+}$ T cell priming by TERS^{cm}-imprinted BMDC may result in facilitation of tumor outgrowth due to local suppression and evasion of immunosurveillance.

Results

To test this *in vivo*, we first utilized an orthotopic tumor model in which C57/BL6 mice are inoculated subcutaneously with murine melanoma B16.F10 tumor cells admixed with TERS^{cm}-imprinted BMDC. Mice injected with this cell mixture displayed accelerated tumor outgrowth, earlier tumor initiation, and decreased survival as compared to mice receiving B16.F10 tumor cells admixed with control BMDC, or tumor cells alone (Fig. 29A), suggesting that TERS polarization of BMDC yields tumor facilitation *in vivo*. To specifically implicate dysfunctional anti-tumor T cell immunity as a mechanism of immune escape, we utilized TRAMP-C1.OVA (TC1.OVA) murine prostate cancer cells that constitutively express OVA, which functions as a strong rejection antigen (120). Whereas no tumors grew in mice receiving TC1.OVA cells alone, transient tumor growth occurred in mice inoculated with TC1.OVA admixed with TERS^{cm}-imprinted BMDC (Fig. 29B). These results indicate that TERS^{cm}-imprinted BMDC inhibit T cell immunity

in vivo, thus promoting tumor growth and even facilitating the take of highly immunogenic tumor cells.

Discussion

The last three previous chapters place into context emerging evidence demonstrating that phenotypically-mature tumor-infiltrating myeloid DC do not efficiently prime T cells despite an activated phenotype, and promote tumor growth via immune evasion. Here, we show that the cell-extrinsic signals deriving from the tumor cell UPR can recapitulate *ab initio* the activated/suppressive phenotype observed in tumor-infiltrating myeloid cells in several *in vivo* systems (74, 75), corroborating the proposal that many of the immune defects observed in the tumor microenvironment may indeed fall under the umbrella of the tumor UPR (121), as implied by an early study showing that silencing *Grp78* in immunogenic mouse fibrosarcoma cells attenuated tumor growth while increasing tumor cell-specific memory $CD8^+$ T cell generation (39).

The tolerogenic ability of DC has been reported in various systems (122). Here we provide evidence for the *ab initio* generation of tolerogenic myeloid DC as a consequence of the cell-extrinsic effects of the tumor UPR. "Classical" tolerogenic DC have been reported to be steady-state immature cells (i.e., cells lacking the expression of costimulatory molecules) able to present antigen, whereas the tolerogenic $TERS^{cm}$-imprinted BMDC described here are phenotypically mature (i.e., express high levels of costimulatory molecules together with antigen presenting molecules) but possess diminished cross-presentation capacity. This paradox can be reconciled by considering that, whereas the basis of "classical" DC tolerogenicity is inadequate maturation resulting

in a costimulatory deficit, $TERS^{cm}$-imprinted BMDC tolerize $CD8^+$ T cells via expression of arginase. Considering the data presented here, the emerging scenario is that, in the context of tumor growth, cell death and antigen release, the occurrence of a tumor UPR remodels the immune microenvironment, creating the conditions for peripheral T cell tolerance which is different from classical low or high antigen dose tolerance, and also tolerance due to defective DC maturation (122). As noted, the effect of TERS on myeloid DC may further direct $CD8^+$ T cells to a regulatory (suppressive) cell fate, hence contributing to the overall pro-tumorigenic characteristic of immune cells in the microenvironment. Thus, the cell-extrinsic effects of the tumor ER stress response constitute a new way through which myeloid DC can hinder $CD8^+$ T cell responses and initiate peripheral T cell tolerance. As the tumor UPR is also a crucial cell-intrinsic mechanism of tumor survival *in vivo*, new forms of therapy targeting its signaling pathways will not only serve to retard tumor cell growth and adaptation, but also diminish tumor-induced immune suppression and peripheral tolerance, which are potential barriers to tumor immunotherapy, providing for a better control of tumor growth by autochthonous or induced anti-tumor T cell responses.

Chapter 5, in part, has been submitted to *Science* under the title, "Cell-extrinsic effects of tumor ER stress imprint myeloid dendritic cells and impair $CD8^+$ T cell priming," authored by, Navin R. Mahadevan, Veronika Anufreichik, Jeffrey Rodvold, Homero Sepulveda, and Maurizio Zanetti. The dissertation author was the primary investigator and author of this paper and the other authors helped perform the research and write the manuscript.

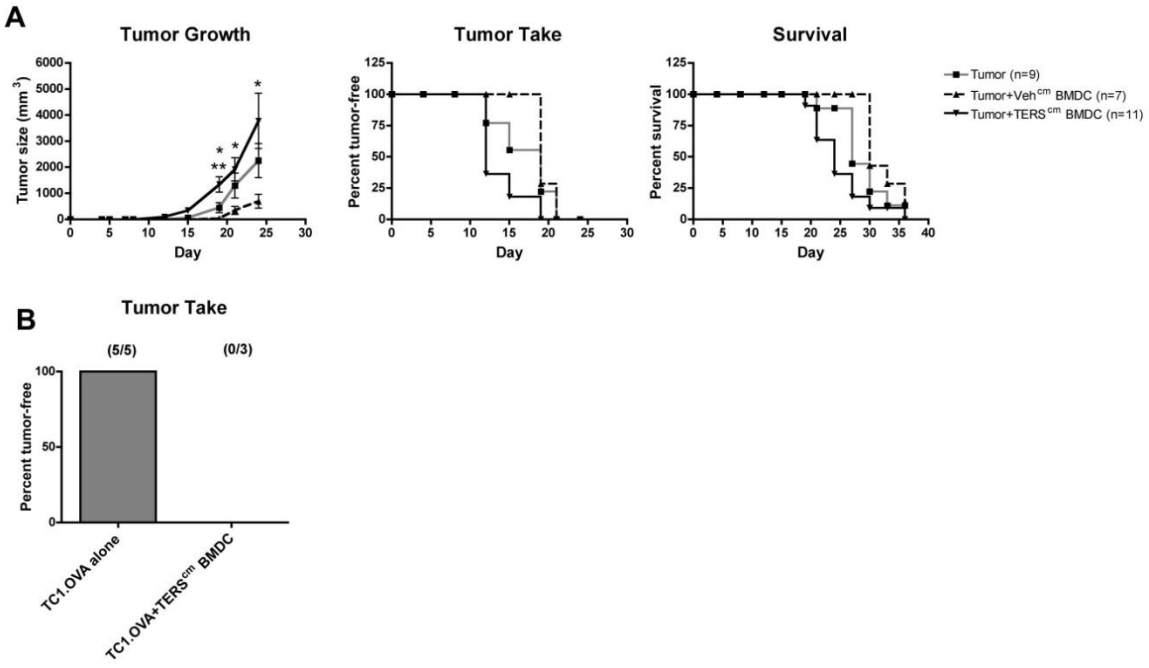

Figure 29. TERS^{cm}-imprinted BMDC promote tumor growth *in vivo*. (A) BMDC were cultured in TERS^{cm} or Veh^{cm} from B16.F10 tumor cells for 24 hours and admixed with B16.F10 cells at a 1:3 ratio (1e4 BMDC:3e4 B16.F10). Admixtures or B16.F10 cells alone (3e4) were injected s.c. into the flanks of C57/BL6 mice and growth monitored by caliper measurement. Tumor size was expressed as volume (mm^3) using the ellipsoid volume formula, V = ½ (H x W^2). Error bars represent SEM of tumor size measurements pooled from all animals in the indicated experimental group. Statistical comparison was made between Tumor+TERS^{cm} BMDC and Tumor alone (top symbols) or Tumor+Veh^{cm} BMDC (bottom symbols) groups on day 19. All other indicated comparisons were made between Tumor+TERS^{cm} BMDC and Tumor+Veh^{cm} BMDC groups. *P < 0.05, **P < 0.01, unpaired, two-tailed t test. **(B)** BMDC were cultured in TERS^{cm} from TC1 tumor cells for 24 hours and admixed with TC1.OVA cells at a 1:3 ratio (1e6 BMDC:3e6 TC1.OVA). Admixtures or TC1.OVA cells alone (3e6) were injected s.c. into the flanks of male C57/BL6 mice and growth monitored by caliper measurement for 22 days.

CONCLUSIONS

The unfolded protein response (UPR) is an adaptive cell signaling pathway that aids eukaryotic cells in coping with conditions in which the protein folding capacity of the endoplasmic reticulum (ER) is saturated or diminished. The tumor microenvironment harbors multiple metabolic ER stressors including low glucose concentrations and hypoxia that induce an ER stress response in tumor cells, which is critical for tumor cell survival, proliferation, and has been correlated with progression. Based on this evidence, the tumor UPR has been most studied as a cell-intrinsic mechanism by which tumor cells survive.

We have found evidence suggesting that the tumor cell UPR can function in a cell-extrinsic manner by transmitting ER stress to myeloid cells that infiltrate the tumor microenvironment, a phenomenon we have termed TERS (transmissible ER stress). TERS-imprinted myeloid cells upregulate production of tumorigenic, inflammatory cytokines but also upregulate immunosuppressive markers, culminating in a pro-inflammatory/suppressive phenotype. Furthermore, these cells display a unique functional phenotype, upregulating costimulatory molecule expression, antigen-presentation machinery, while downregulating effective high-affinity antigen cross-presentation.

Importantly, TERS-imprinted BMDC do not effectively prime $CD8^+$ T cells, causing activation without proliferation, in part due to increased arginase activity. Additionally, $CD8^+$ T cells cross-primed by TERS-imprinted BMDC display a regulatory phenotype and abnormally highly splicing of *Xbp-1*. We also show that TERS-imprinted BMDC can also dominantly suppress the proper cross-priming function of normal

bystander BMDC. Lastly, TERS-imprinted BMDC facilitate tumor growth in vivo, even promoting the transient escape of highly immunogenic tumor cells.

Taken together, we demonstrate for the first time the *ab initio* generation of tumor-imprinted myeloid cells that have many of the characteristics of previously-described tumor-infiltrating myeloid cells and bring to the forefront the tumor UPR as a fundamental driver of this polarization. A schematic of the current understanding of the interaction between tumor cells and the immune system, as well as the proposed TERS-mediated tumor-myeloid cell interaction and its consequences on anti-tumor immunity is diagrammed in Figure 30.

In the clinical setting, autochthonous and vaccine-induced T cell responses against cancer are locally hampered by the immunosuppressive microenvironment enforced by the tumor. The results here described indicate that through its cell-extrinsic effects on myeloid cells, and consequently, T cells, the tumor UPR could be a key mediator in the establishment of such an environment. Looking forward, effective therapy and immunotherapy against tumors will need to incorporate agents that help remodel the immune landscape of the tumor microenvironment in favor of immunity; disabling the tumor UPR would be one such mechanism. Anti-tumor UPR therapy would have two added benefits: 1) reducing the tumorigenic, proinflammatory signaling intimately associated with the UPR, and, 2) as the tumor UPR is a key cell-intrinsic regulator of tumor cell survival, its inhibition would also curb tumor adaptation and survival to microenvironmental *noxae*.

The Conclusions section, in part, has been published in the manuscript: Mahadevan, N.R. and Zanetti, M. Tumor stress inside out: Cell-extrinsic effects of the

unfolded protein response in tumor cells modulate the immunological landscape of the tumor microenvironment. *J Immunol* 187(9):4403-9, 2011. The dissertation author was the primary author of this paper.

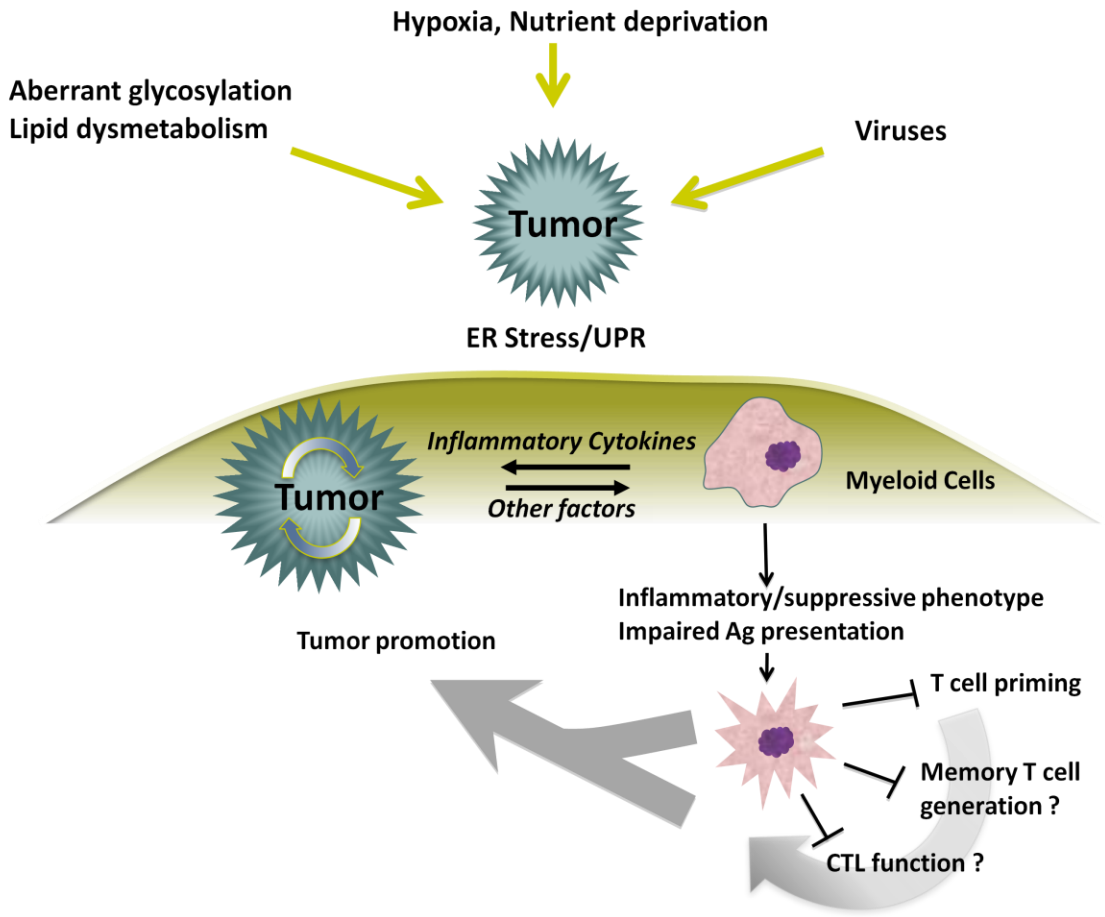

Figure 30. Relationships linking various ER stressors, the UPR, tumor cells, and immune cells in the microenvironment. The umbrella (green shading) represents the multifaceted influence of tumor ER stress/UPR on myeloid cells and elements of the adaptive T cell response. In this new framework, the UPR acts as a cell-intrinsic tumor prosurvival factor (circular arrow). ER-stressed tumor cells also may secrete cytokines and other factors that harness myeloid cells in the tumor microenvironment, imprinting them with an inflammatory/suppressive phenotype (see text for description) that facilitates tumor growth via T cell-dependent and -independent mechanisms (merging arrows).

APPENDIX. MATERIALS AND METHODS

Mice, Preparation of BMDM/BMDC, and Cell Culture Procedures

C57BL/6 mice were purchased from Charles River and housed at the Moore's Cancer Center Animal Facility. TLR2 KO and TLR4 KO mice were the kind gift of Drs. M. Karin and M. Corr, respectively (University of California, San Diego) with permission from Dr. S. Akira. All mice were handled in accordance with University of California, San Diego Animal Subjects Program Guidelines. Femurs, tibias, and fibulas from $IL6R^{-/-}$ mice (123) were contributed by Dr. A Drew (University of Cincinnati). Bone marrow cells were flushed from the femurs and cultured for 7 days in 30% L929 cell-conditioned medium (124) to obtain bone marrow-derived macrophages (BMDM). The yield of $CD11b^{+}$ macrophages was >95%. To obtain BMDC, bone marrow cells from C57/BL6 mice were flushed from femurs and tibias in cold, unsupplemented RPMI 1640. After RBC lysis, bone marrow cells were cultured for 6 days in complete RPMI medium containing 10% v/v supernatant from mGMCSF-producing hybridoma cells (GCM, courtesy R. Steinman). Every two days, cells were washed and resupplemented with complete RPMI containing 10% GCM, yielding >85% immature $CD11b^{+}/CD11c^{+}$ myeloid BMDC on day 6.

TRAMP-C1, B16.F10, and LLC cells were originally obtained from Drs. A. Weinberg (Providence Portland Medical Center, OR), D. Carson, and J. Varner (University of California, San Diego), respectively. J774 cells were a kind gift from Drs. A. Timmer and V. Nizet (University of California, San Diego). All lines were grown under standard conditions in RPMI medium 1640 or DMEM (Mediatech) supplemented

with HEPES buffer, L-glutamine, sodium pyruvate, MEM non-essential amino acids (Gibco), Penicillin/Streptomycin, 2-mercaptoethanol and 10% FBS (Hyclone: Lot No. KSJ30470 with an LPS content < 0.06 EU/mL by LAL test) at 37°C in 5% CO_2 atmosphere, except for addition of conditioned media. All cells were routinely tested for mycoplasma using the luminescence-based MycoAlert kit (Lonza), and confirmed to be mycoplasma free.

Conditioned Media

ER stress conditioned medium was generated as follows. Briefly, tumor cells were induced to undergo ER stress by culture in thapsigargin (Tg) (Enzo Life Sciences; > 99% pure by HPLC) (300 nM) for 2 hrs. Control cells were similarly treated with an equal volume of vehicle (100% ethanol). Cells were washed 2x with Dulbecco's phosphate-buffered saline (Mediatech), and then incubated in fresh medium for 16 hrs. Conditioned medium was centrifuged for 10 minutes at 2,000 rpm and then filtered through a 0.22 μm filter (Millipore). Conditioned medium from apoptotic or control cells was generated from TC1 cells treated with 100 nM staurosporine (Sigma) or vehicle (DMSO), respectively. To generate glucose-deprived tumor conditioned medium, tumor cells were cultured for 24 h in basal RPMI 1640 or DMEM lacking glucose supplemented with 10% dialyzed FBS (10000 MWCO, HyClone), L-glutamine, and penicillin/streptomycin. Conditioned medium was harvested, centrifuged at 2000 rpm for 10 minutes, and passed through a 0.22 μm syringe filter (Millipore) before use. J774 macrophages and BMDM were incubated in the appropriate conditioned and control media for the times indicated. For experiments in which we probed synergy between ER

stress conditioned medium and TLR4 signaling, macrophages were incubated in ER stress or vehicle control conditioned medium with or without bacterial lipopolysaccharide (LPS) (Sigma Cat. # L2654) at a final concentration of 100 ng/mL. For heat inactivation experiments, basal medium and tumor cell conditioned media were heated to 37 ºC, 56 ºC, or 95 ºC for 30 minutes. Before addition to macrophages, heated media were briefly cooled on ice to room temperature.

Mass Spectroscopy

Thapsigargin in culture media was quantified by LC/MS/MS after sample clean-up by solid phase extraction (Supelco 52611-U, DSC-18T, 100mg). Tg was isolated by reversed-phase C-18 HPLC using gradient elution with up to 95% methanol:5% 0.1% formic acid in water. Quantitation was based on peak area generated by scanning for cumulative product ions (m/z 513, 573, 612) from the protonated molecular ion parent (m/z 674). External standardization was employed, utilizing Excalibur Version 2.0 Software, interfaced with a Thermo-Finnigan LCQ DUO mass spectrometer and Thermo-Fisher Surveyor P5000 HPLC and Autosampler modules.

Injection of Tumor ER Stress Conditioned Media *In Vivo*

10 mL of Tg conditioned medium or EtOH vehicle control medium from TC1, B16.F10, and LLC tumor cells, were concentrated by lyophilization for 24-36 hrs, resuspended in 1 mL sterile, DNA/RNA-free water (Mediatech), centrifuged for 5 minutes at 13000 rpm, and the supernatant aspirated in a 1 mL sterile syringe. 14-18 week old C57BL/6 mice were injected i.p. with (*i*) 10x tumor ER stress conditioned

medium, (*ii*) 10x vehicle control medium or (*iii*) tunicamycin (2 mg/kg) in a final volume of 1 mL dPBS. Eight hrs later, mice were euthanized, livers surgically removed and passed through a 40 μm cell strainer. Liver samples were washed once in dPBS, aliquoted for RNA isolation, and gene expression quantified by qPCR as described below.

BMDC Cross Presentation and T Cell Coculture

BMDC were first exposed to tumor ER-stressed c.m. or control media for 8 h after which heat-treated ovalbumin (1 mg/mL) (Sigma) was added to cultures for a further 16 h. $CD8^+$ T cells were negatively selected (StemCell Tech) from a spleen/lymph nodes cell suspension from OT-I/$Rag^{-/-}$ mice (graciously provided by Dr. S. Schoenberger and Dr. J Chang) and the yield of transgenic cells was determined by enumeration of $Va2^+/CD8^+$ cells by flow cytometry, which was >90%. 2.5E5 $Va2^+/CD8^+$ T cells were then co-cultured with 1E5 BMDC for 96 h. In some cases, negatively selected $CD8^+$ cells were labeled with 0.5 μM CFDA-SE (Invitrogen) before co-culture. For exogenous antigen rescue experiments, TERS-treated BMDC were pulsed with indicated concentrations of SIINFEKL peptide for 4 hours at 37 °C prior to co-culture. For arginase inhibition experiments, 2 mM L-arginine (EMD Chemicals) or 10 mM L-norvaline (EMD Chemicals) were added to cell culture medium prior to addition of BMDC and T cells. For anergy experiments, indicated concentrations of recombinant mouse IL-2 (R&D Systems) were added to cell culture medium prior to addition of BMDC and T cells.

Quantitative RT-PCR (qPCR)

RNA was isolated from cells using the RNeasy (Qiagen), RNeasy Plus (Qiagen), or Nucleospin II kits (Macherey-Nagel). Concentration and purity of RNA was determined by analysis on a NanoDrop spectrophotometer (Thermo Scientific). cDNA was obtained using the High Capacity cDNA Synthesis kit (Life Technologies/Applied Biosystems) and quantitative PCR was performed on an ABI StepOne system using TaqMan reagents for 50 cycles using universal cycling conditions. Target gene expression was normalized to β-actin, and analyzed using the –ΔΔCt relative quantification method. Validated FAM-labeled mouse *Il-23p19(a), Il-6, Tnf, Il-17a, Il-10, Tgf-β, FoxP3, Ddit3 (Chop), Myd116 (Gadd34), Hspa5 (Grp78), Arg1* and VIC-labeled mouse β-actin TaqMan primer/probe sets (Life Technologies/Applied Biosystems) were used. For macrophage experiments, mouse *Xbp-1* FAM-labeled qPCR probe/primer sets was obtained from Integrated DNA Technologies. For gel-based PCR, Xbp-1 amplicons were amplified using the following cycling conditions: 96°C for 2 min., followed by 30 cycles of 96°C for 30 s, 60°C for 30 s, 72°C for 30 s. and a 1 min 72°C extension, resolved on a 2.5% agarose gel, and imaged using a BioRad GelDoc system. The list of primers is shown below. For dendritic cell experiments, FAM-labeled qPCR probe/primer sets specific for mouse *Xbp-1s* (IDT Technologies) were used

m*Xbp-1*	Forward	5’-ACACGCTTGGGAATGGACAC-3’
	Reverse	5’-CCATGGGAAGATGTTCTGGG-3’

m*Gapdh*	Forward	5'-ACGGATTTGGTCGTATTGGGC-3'
	Reverse	5'-TTGACGGTGCCATGGAATTTG-3'
m*Xbp-1* (qPCR)	1	5'-ACCAGGAGTTAAGAACACGC-3'
	2	5'-CAACAGTGTCAGAGTCCATGG-3'
	Probe	5'-AGGTGCAGGCCCAGTTGTCA-3'

Flow Cytometry

Single cell suspensions were stained with fluorochrome-labeled anti-CD86 (BD Pharmingen, clone GL1), anti-CD80 (BD Pharmingen, clone 16-10-A1), anti-CD40 (BD Pharmingen, clone 3/23), anti-CD64 (BD Biosciences, clone X54-5/7.1), anti-CD16/32 (BD Biosciences, clone 2.4G2), anti-CD14 (BD Biosciences, clone rmC5-3), anti-CD11b (eBioscience, clone M1/70), anti-CD11c (eBioscience, clone N418), anti-$H2k^b$ (BD Pharmingen, clone AF6-88.5), anti-IA^b (BD Pharmingen, clone AF6-120.1), anti-K^b-SIINFEKL (eBioscience, clone ebio25.D1.16), anti-PDL-1 (BD Pharmingen, clone MIH5), anti-CD8α (eBioscience, clone Ly-2), anti-Vα2 (BD Pharmingen, clone B20.1), anti-CD69 (BD Pharmingen, clone H12F3), anti-CD25 (BD Pharmingen, clone PC61.5), anti-CD62L (BD Pharmingen, clone MEL14), anti-CD44 (BD Pharmingen, clone IM7), anti-IFN-γ (BD Pharmingen, clone XMG1.2), anti-PD-1 (BD Pharmingen, clone RMP1-30), anti-CD28 (BD Pharmingen, clone 37.51) and Annexin V (BD Pharmingen) antibodies, or appropriate isotype controls. Viability was determined by 7-AAD (CalBiochem) exclusion. For cell cyle analysis, $CD8^+$ cells were fixed in 70% ice-cold ethanol for one hour and then for 24 hours at -20 °C. Cells were incubated in 7-AAD (25

μg/mL) and RNase A (100 μg/mL) for 30 minutes at 37 °C. A FACSCalibur cytometer (Becton&Dickinson) was used for acquisition of data, and CellQuest Pro (BD Biosciences) and FlowJo software (Tree Star) were used for data analysis.

Multiplex Cytometric Bead Assay

BD™ CBA Flex set assays were used to measure mouse IL-6, IL-23, TNF-α, IL-10, MIP-1α, MIP-1β, and MCP-1 (BD Pharmingen). Briefly, each capture bead is a single population with distinct fluorescence intensity and is coated with a capture antibody specific for each of the soluble proteins. The bead population is resolvable in the NIR and Red channels of a BD FACSArray™ bioanalyzer flow cytometer. Each bead population is given an alphanumeric position designation indicating its position relative to other beads in the BD CBA Flex Set system. Beads with different positions can be combined in assays to create a multiplex assay. In a BD CBA Flex Set assay the capture bead, PE-conjugated detection reagent, and standard or test samples are incubated together to form sandwich complexes. Following acquisition of sample data using the flow cytometer, the sample results are generated in graphical and tabular formats using the FCAP Array™ Software.

***In vivo* Tumor Studies**

BMDC were exposed to ER-stressed tumor c.m. or unstressed tumor c.m. for 24 h. Tumor cells and BMDC were harvested and washed twice with dPBS-. Tumor cells were admixed with BMDC at a 3:1 ratio (3e4 B16.F10:1e4 BMDC or 3e6 TC1.OVA:1e6 BMDC) and injected s.c. into 6-10 week-old C57/BL6 mice. Experiments using

TC1.OVA cells were conducted using male mice only. Tumor growth was measured by taking two-dimensional caliper measurements starting 4 days after injection until tumors reached ≥20 mm in one dimension, at which time the mice were sacrificed in accordance with UCSD animal welfare standards. Tumor size was expressed as volume (mm^3) using the ellipsoid volume formula, $V = ½ (H \times W^2)$.

REFERENCES

1. Virchow, R. K. L. 1865. *Die Krankhaften Geschwülste* A. Hirschwald, Berlin.

2. Schreiber, R. D., L. J. Old, and M. J. Smyth. 2011. Cancer immunoediting: integrating immunity's roles in cancer suppression and promotion. *Science* 331:1565-1570.

3. Mumm, J. B., and M. Oft. 2008. Cytokine-based transformation of immune surveillance into tumor-promoting inflammation. *Oncogene* 27:5913-5919.

4. Badovinac, V. P., K. A. Messingham, A. Jabbari, J. S. Haring, and J. T. Harty. 2005. Accelerated CD8+ T-cell memory and prime-boost response after dendritic-cell vaccination. *Nat Med* 11:748-756.

5. Feldman, D. E., V. Chauhan, and A. C. Koong. 2005. The unfolded protein response: a novel component of the hypoxic stress response in tumors. *Mol Cancer Res* 3:597-605.

6. Harding, H. P., M. Calfon, F. Urano, I. Novoa, and D. Ron. 2002. Transcriptional and translational control in the Mammalian unfolded protein response. *Annu Rev Cell Dev Biol* 18:575-599.

7. Schroder, M., and R. J. Kaufman. 2005. ER stress and the unfolded protein response. *Mutat Res* 569:29-63.

8. Bertolotti, A., Y. Zhang, L. M. Hendershot, H. P. Harding, and D. Ron. 2000. Dynamic interaction of BiP and ER stress transducers in the unfolded-protein response. *Nat Cell Biol* 2:326-332.

9. Yoshida, H., T. Matsui, A. Yamamoto, T. Okada, and K. Mori. 2001. XBP1 mRNA is induced by ATF6 and spliced by IRE1 in response to ER stress to produce a highly active transcription factor. *Cell* 107:881-891.

10. Lee, A. H., N. N. Iwakoshi, and L. H. Glimcher. 2003. XBP-1 regulates a subset of endoplasmic reticulum resident chaperone genes in the unfolded protein response. *Mol Cell Biol* 23:7448-7459.

11. Yamamoto, K., T. Sato, T. Matsui, M. Sato, T. Okada, H. Yoshida, A. Harada, and K. Mori. 2007. Transcriptional induction of mammalian ER quality control proteins is mediated by single or combined action of ATF6alpha and XBP1. *Dev Cell* 13:365-376.

12. Harding, H. P., Y. Zhang, and D. Ron. 1999. Protein translation and folding are coupled by an endoplasmic-reticulum-resident kinase. *Nature* 397:271-274.

13. Zinszner, H., M. Kuroda, X. Wang, N. Batchvarova, R. T. Lightfoot, H. Remotti, J. L. Stevens, and D. Ron. 1998. CHOP is implicated in programmed cell death in response to impaired function of the endoplasmic reticulum. *Genes Dev* 12:982-995.

14. Heazlewood, C. K., M. C. Cook, R. Eri, G. R. Price, S. B. Tauro, D. Taupin, D. J. Thornton, C. W. Png, T. L. Crockford, R. J. Cornall, R. Adams, M. Kato, K. A. Nelms, N. A. Hong, T. H. Florin, C. C. Goodnow, and M. A. McGuckin. 2008. Aberrant mucin assembly in mice causes endoplasmic reticulum stress and spontaneous inflammation resembling ulcerative colitis. *PLoS Med* 5:e54.

15. Little, J. L., F. B. Wheeler, D. R. Fels, C. Koumenis, and S. J. Kridel. 2007. Inhibition of fatty acid synthase induces endoplasmic reticulum stress in tumor cells. *Cancer Res* 67:1262-1269.

16. He, B. 2006. Viruses, endoplasmic reticulum stress, and interferon responses. *Cell Death Differ* 13:393-403.

17. Drogat, B., P. Auguste, D. T. Nguyen, M. Bouchecareilh, R. Pineau, J. Nalbantoglu, R. J. Kaufman, E. Chevet, A. Bikfalvi, and M. Moenner. 2007. IRE1 signaling is essential for ischemia-induced vascular endothelial growth factor-A expression and contributes to angiogenesis and tumor growth in vivo. *Cancer Res* 67:6700-6707.

18. Romero-Ramirez, L., H. Cao, D. Nelson, E. Hammond, A. H. Lee, H. Yoshida, K. Mori, L. H. Glimcher, N. C. Denko, A. J. Giaccia, Q. T. Le, and A. C. Koong. 2004. XBP1 is essential for survival under hypoxic conditions and is required for tumor growth. *Cancer Res* 64:5943-5947.

19. Bi, M., C. Naczki, M. Koritzinsky, D. Fels, J. Blais, N. Hu, H. Harding, I. Novoa, M. Varia, J. Raleigh, D. Scheuner, R. J. Kaufman, J. Bell, D. Ron, B. G. Wouters, and C. Koumenis. 2005. ER stress-regulated translation increases tolerance to extreme hypoxia and promotes tumor growth. *EMBO J* 24:3470-3481.

20. Paudyal, B., N. Oriuchi, P. Paudyal, T. Higuchi, T. Nakajima, and K. Endo. 2008. Expression of glucose transporters and hexokinase II in cholangiocellular carcinoma compared using [18F]-2-fluro-2-deoxy-D-glucose positron emission tomography. *Cancer Sci* 99:260-266.

21. Paudyal, B., P. Paudyal, N. Oriuchi, Y. Tsushima, T. Nakajima, and K. Endo. 2008. Clinical implication of glucose transport and metabolism evaluated by 18F-FDG PET in hepatocellular carcinoma. *Int J Oncol* 33:1047-1054.

22. Kunkel, M., T. E. Reichert, P. Benz, H. A. Lehr, J. H. Jeong, S. Wieand, P. Bartenstein, W. Wagner, and T. L. Whiteside. 2003. Overexpression of Glut-1

and increased glucose metabolism in tumors are associated with a poor prognosis in patients with oral squamous cell carcinoma. *Cancer* 97:1015-1024.

23. Ong, L. C., Y. Jin, I. C. Song, S. Yu, K. Zhang, and P. K. Chow. 2008. 2-[18F]-2-deoxy-D-glucose (FDG) uptake in human tumor cells is related to the expression of GLUT-1 and hexokinase II. *Acta Radiol* 49:1145-1153.

24. Scriven, P., N. J. Brown, A. G. Pockley, and L. Wyld. 2007. The unfolded protein response and cancer: a brighter future unfolding? *J Mol Med* 85:331-341.

25. Henning, T., M. Kraus, M. Brischwein, A. M. Otto, and B. Wolf. 2004. Relevance of tumor microenvironment for progression, therapy and drug development. *Anticancer Drugs* 15:7-14.

26. Mueller-Klieser, W., P. Vaupel, and R. Manz. 1983. Tumour oxygenation under normobaric and hyperbaric conditions. *Br J Radiol* 56:559-564.

27. Shiu, R. P., J. Pouyssegur, and I. Pastan. 1977. Glucose depletion accounts for the induction of two transformation-sensitive membrane proteinsin Rous sarcoma virus-transformed chick embryo fibroblasts. *Proc Natl Acad Sci U S A* 74:3840-3844.

28. Park, H. R., A. Tomida, S. Sato, Y. Tsukumo, J. Yun, T. Yamori, Y. Hayakawa, T. Tsuruo, and K. Shin-ya. 2004. Effect on tumor cells of blocking survival response to glucose deprivation. *J Natl Cancer Inst* 96:1300-1310.

29. Saito, S., A. Furuno, J. Sakurai, A. Sakamoto, H. R. Park, K. Shin-Ya, T. Tsuruo, and A. Tomida. 2009. Chemical genomics identifies the unfolded protein response as a target for selective cancer cell killing during glucose deprivation. *Cancer Res* 69:4225-4234.

30. Ye, J., M. Kumanova, L. S. Hart, K. Sloane, H. Zhang, D. N. De Panis, E. Bobrovnikova-Marjon, J. A. Diehl, D. Ron, and C. Koumenis. 2010. The GCN2-ATF4 pathway is critical for tumour cell survival and proliferation in response to nutrient deprivation. *EMBO J* 29:2082-2096.

31. Spiotto, M. T., A. Banh, I. Papandreou, H. Cao, M. G. Galvez, G. C. Gurtner, N. C. Denko, Q. T. Le, and A. C. Koong. 2010. Imaging the unfolded protein response in primary tumors reveals microenvironments with metabolic variations that predict tumor growth. *Cancer Res* 70:78-88.

32. Fernandez, P. M., S. O. Tabbara, L. K. Jacobs, F. C. Manning, T. N. Tsangaris, A. M. Schwartz, K. A. Kennedy, and S. R. Patierno. 2000. Overexpression of the glucose-regulated stress gene GRP78 in malignant but not benign human breast lesions. *Breast Cancer Res Treat* 59:15-26.

33. Uramoto, H., K. Sugio, T. Oyama, S. Nakata, K. Ono, T. Yoshimastu, M. Morita, and K. Yasumoto. 2005. Expression of endoplasmic reticulum molecular chaperone Grp78 in human lung cancer and its clinical significance. *Lung Cancer* 49:55-62.

34. Shuda, M., N. Kondoh, N. Imazeki, K. Tanaka, T. Okada, K. Mori, A. Hada, M. Arai, T. Wakatsuki, O. Matsubara, N. Yamamoto, and M. Yamamoto. 2003. Activation of the ATF6, XBP1 and grp78 genes in human hepatocellular carcinoma: a possible involvement of the ER stress pathway in hepatocarcinogenesis. *J Hepatol* 38:605-614.

35. Xing, X., M. Lai, Y. Wang, E. Xu, and Q. Huang. 2006. Overexpression of glucose-regulated protein 78 in colon cancer. *Clin Chim Acta* 364:308-315.

36. Daneshmand, S., M. L. Quek, E. Lin, C. Lee, R. J. Cote, D. Hawes, J. Cai, S. Groshen, G. Lieskovsky, D. G. Skinner, A. S. Lee, and J. Pinski. 2007. Glucose-regulated protein GRP78 is up-regulated in prostate cancer and correlates with recurrence and survival. *Hum Pathol* 38:1547-1552.

37. Pyrko, P., A. H. Schonthal, F. M. Hofman, T. C. Chen, and A. S. Lee. 2007. The unfolded protein response regulator GRP78/BiP as a novel target for increasing chemosensitivity in malignant gliomas. *Cancer Res* 67:9809-9816.

38. Zhuang, L., R. A. Scolyer, C. S. Lee, S. W. McCarthy, W. A. Cooper, X. D. Zhang, J. F. Thompson, and P. Hersey. 2009. Expression of glucose-regulated stress protein GRP78 is related to progression of melanoma. *Histopathology* 54:462-470.

39. Jamora, C., G. Dennert, and A. S. Lee. 1996. Inhibition of tumor progression by suppression of stress protein GRP78/BiP induction in fibrosarcoma B/C10ME. *Proc Natl Acad Sci U S A* 93:7690-7694.

40. Dong, D., M. Ni, J. Li, S. Xiong, W. Ye, J. J. Virrey, C. Mao, R. Ye, M. Wang, L. Pen, L. Dubeau, S. Groshen, F. M. Hofman, and A. S. Lee. 2008. Critical role of the stress chaperone GRP78/BiP in tumor proliferation, survival, and tumor angiogenesis in transgene-induced mammary tumor development. *Cancer Res* 68:498-505.

41. Fu, Y., S. Wey, M. Wang, R. Ye, C. P. Liao, P. Roy-Burman, and A. S. Lee. 2008. Pten null prostate tumorigenesis and AKT activation are blocked by targeted knockout of ER chaperone GRP78/BiP in prostate epithelium. *Proc Natl Acad Sci U S A* 105:19444-19449.

42. Romero-Ramirez, L., H. Cao, M. P. Regalado, N. Kambham, D. Siemann, J. J. Kim, Q. T. Le, and A. C. Koong. 2009. X box-binding protein 1 regulates angiogenesis in human pancreatic adenocarcinomas. *Transl Oncol* 2:31-38.

43. Blais, J. D., C. L. Addison, R. Edge, T. Falls, H. Zhao, K. Wary, C. Koumenis, H. P. Harding, D. Ron, M. Holcik, and J. C. Bell. 2006. Perk-dependent translational regulation promotes tumor cell adaptation and angiogenesis in response to hypoxic stress. *Mol Cell Biol* 26:9517-9532.

44. Healy, S. J., A. M. Gorman, P. Mousavi-Shafaei, S. Gupta, and A. Samali. 2009. Targeting the endoplasmic reticulum-stress response as an anticancer strategy. *Eur J Pharmacol* 625:234-246.

45. Lee, A. H., N. N. Iwakoshi, K. C. Anderson, and L. H. Glimcher. 2003. Proteasome inhibitors disrupt the unfolded protein response in myeloma cells. *Proc Natl Acad Sci U S A* 100:9946-9951.

46. Bonizzi, G., and M. Karin. 2004. The two NF-kappaB activation pathways and their role in innate and adaptive immunity. *Trends Immunol* 25:280-288.

47. Deng, J., P. D. Lu, Y. Zhang, D. Scheuner, R. J. Kaufman, N. Sonenberg, H. P. Harding, and D. Ron. 2004. Translational repression mediates activation of nuclear factor kappa B by phosphorylated translation initiation factor 2. *Mol Cell Biol* 24:10161-10168.

48. Jiang, H. Y., S. A. Wek, B. C. McGrath, D. Scheuner, R. J. Kaufman, D. R. Cavener, and R. C. Wek. 2003. Phosphorylation of the alpha subunit of eukaryotic initiation factor 2 is required for activation of NF-kappaB in response to diverse cellular stresses. *Mol Cell Biol* 23:5651-5663.

49. Hu, P., Z. Han, A. D. Couvillon, R. J. Kaufman, and J. H. Exton. 2006. Autocrine tumor necrosis factor alpha links endoplasmic reticulum stress to the membrane death receptor pathway through IRE1alpha-mediated NF-kappaB activation and down-regulation of TRAF2 expression. *Mol Cell Biol* 26:3071-3084.

50. Yamazaki, H., N. Hiramatsu, K. Hayakawa, Y. Tagawa, M. Okamura, R. Ogata, T. Huang, S. Nakajima, J. Yao, A. W. Paton, J. C. Paton, and M. Kitamura. 2009. Activation of the Akt-NF-kappaB pathway by subtilase cytotoxin through the ATF6 branch of the unfolded protein response. *J Immunol* 183:1480-1487.

51. Luo, D., Y. He, H. Zhang, L. Yu, H. Chen, Z. Xu, S. Tang, F. Urano, and W. Min. 2008. AIP1 is critical in transducing IRE1-mediated endoplasmic reticulum stress response. *J Biol Chem* 283:11905-11912.

52. Urano, F., X. Wang, A. Bertolotti, Y. Zhang, P. Chung, H. P. Harding, and D. Ron. 2000. Coupling of stress in the ER to activation of JNK protein kinases by transmembrane protein kinase IRE1. *Science* 287:664-666.

53. Xue, X., J. H. Piao, A. Nakajima, S. Sakon-Komazawa, Y. Kojima, K. Mori, H. Yagita, K. Okumura, H. Harding, and H. Nakano. 2005. Tumor necrosis factor alpha (TNFalpha) induces the unfolded protein response (UPR) in a reactive oxygen species (ROS)-dependent fashion, and the UPR counteracts ROS accumulation by TNFalpha. *J Biol Chem* 280:33917-33925.

54. Zhang, K., X. Shen, J. Wu, K. Sakaki, T. Saunders, D. T. Rutkowski, S. H. Back, and R. J. Kaufman. 2006. Endoplasmic reticulum stress activates cleavage of CREBH to induce a systemic inflammatory response. *Cell* 124:587-599.

55. Sulciner, D. J., K. Irani, Z. X. Yu, V. J. Ferrans, P. Goldschmidt-Clermont, and T. Finkel. 1996. rac1 regulates a cytokine-stimulated, redox-dependent pathway necessary for NF-kappaB activation. *Mol Cell Biol* 16:7115-7121.

56. Cullinan, S. B., and J. A. Diehl. 2006. Coordination of ER and oxidative stress signaling: the PERK/Nrf2 signaling pathway. *Int J Biochem Cell Biol* 38:317-332.

57. Malhotra, J. D., and R. J. Kaufman. 2007. Endoplasmic reticulum stress and oxidative stress: a vicious cycle or a double-edged sword? *Antioxid Redox Signal* 9:2277-2293.

58. Malhotra, J. D., H. Miao, K. Zhang, A. Wolfson, S. Pennathur, S. W. Pipe, and R. J. Kaufman. 2008. Antioxidants reduce endoplasmic reticulum stress and improve protein secretion. *Proc Natl Acad Sci U S A* 105:18525-18530.

59. Mantovani, A., S. Sozzani, M. Locati, P. Allavena, and A. Sica. 2002. Macrophage polarization: tumor-associated macrophages as a paradigm for polarized M2 mononuclear phagocytes. *Trends Immunol* 23:549-555.

60. Kusmartsev, S., and D. I. Gabrilovich. 2006. Role of immature myeloid cells in mechanisms of immune evasion in cancer. *Cancer Immunol Immunother* 55:237-245.

61. Sica, A., and V. Bronte. 2007. Altered macrophage differentiation and immune dysfunction in tumor development. *J Clin Invest* 117:1155-1166.

62. Kusmartsev, S., Y. Nefedova, D. Yoder, and D. I. Gabrilovich. 2004. Antigen-specific inhibition of CD8+ T cell response by immature myeloid cells in cancer is mediated by reactive oxygen species. *J Immunol* 172:989-999.

63. Huang, B., P. Y. Pan, Q. Li, A. I. Sato, D. E. Levy, J. Bromberg, C. M. Divino, and S. H. Chen. 2006. Gr-1+CD115+ immature myeloid suppressor cells mediate the development of tumor-induced T regulatory cells and T-cell anergy in tumor-bearing host. *Cancer Res* 66:1123-1131.

64. Chaux, P., N. Favre, M. Martin, and F. Martin. 1997. Tumor-infiltrating dendritic cells are defective in their antigen-presenting function and inducible B7 expression in rats. *Int J Cancer* 72:619-624.

65. Ostrand-Rosenberg, S., and P. Sinha. 2009. Myeloid-derived suppressor cells: linking inflammation and cancer. *J Immunol* 182:4499-4506.

66. Almand, B., J. I. Clark, E. Nikitina, J. van Beynen, N. R. English, S. C. Knight, D. P. Carbone, and D. I. Gabrilovich. 2001. Increased production of immature myeloid cells in cancer patients: a mechanism of immunosuppression in cancer. *J Immunol* 166:678-689.

67. Gabrilovich, D. I., H. L. Chen, K. R. Girgis, H. T. Cunningham, G. M. Meny, S. Nadaf, D. Kavanaugh, and D. P. Carbone. 1996. Production of vascular endothelial growth factor by human tumors inhibits the functional maturation of dendritic cells. *Nat Med* 2:1096-1103.

68. Bunt, S. K., L. Yang, P. Sinha, V. K. Clements, J. Leips, and S. Ostrand-Rosenberg. 2007. Reduced inflammation in the tumor microenvironment delays the accumulation of myeloid-derived suppressor cells and limits tumor progression. *Cancer Res* 67:10019-10026.

69. Song, X., Y. Krelin, T. Dvorkin, O. Bjorkdahl, S. Segal, C. A. Dinarello, E. Voronov, and R. N. Apte. 2005. CD11b+/Gr-1+ immature myeloid cells mediate suppression of T cells in mice bearing tumors of IL-1beta-secreting cells. *J Immunol* 175:8200-8208.

70. Rodriguez, P. C., C. P. Hernandez, D. Quiceno, S. M. Dubinett, J. Zabaleta, J. B. Ochoa, J. Gilbert, and A. C. Ochoa. 2005. Arginase I in myeloid suppressor cells is induced by COX-2 in lung carcinoma. *J Exp Med* 202:931-939.

71. Sinha, P., V. K. Clements, A. M. Fulton, and S. Ostrand-Rosenberg. 2007. Prostaglandin E2 promotes tumor progression by inducing myeloid-derived suppressor cells. *Cancer Res* 67:4507-4513.

72. Otsuji, M., Y. Kimura, T. Aoe, Y. Okamoto, and T. Saito. 1996. Oxidative stress by tumor-derived macrophages suppresses the expression of CD3 zeta chain of T-cell receptor complex and antigen-specific T-cell responses. *Proc Natl Acad Sci U S A* 93:13119-13124.

73. Ataera, H., E. Hyde, K. M. Price, P. Stoitzner, and F. Ronchese. 2011. Murine Melanoma-Infiltrating Dendritic Cells Are Defective in Antigen Presenting Function Regardless of the Presence of CD4CD25 Regulatory T Cells. *PLoS One* 6:e17515.

74. Liu, Q., C. Zhang, A. Sun, Y. Zheng, L. Wang, and X. Cao. 2009. Tumor-educated CD11bhighIalow regulatory dendritic cells suppress T cell response through arginase I. *J Immunol* 182:6207-6216.

75. Norian, L. A., P. C. Rodriguez, L. A. O'Mara, J. Zabaleta, A. C. Ochoa, M. Cella, and P. M. Allen. 2009. Tumor-infiltrating regulatory dendritic cells inhibit CD8+ T cell function via L-arginine metabolism. *Cancer Res* 69:3086-3094.

76. Stoitzner, P., L. K. Green, J. Y. Jung, K. M. Price, H. Atarea, B. Kivell, and F. Ronchese. 2008. Inefficient presentation of tumor-derived antigen by tumor-infiltrating dendritic cells. *Cancer Immunol Immunother* 57:1665-1673.

77. Van Ginderachter, J. A., K. Movahedi, G. Hassanzadeh Ghassabeh, S. Meerschaut, A. Beschin, G. Raes, and P. De Baetselier. 2006. Classical and alternative activation of mononuclear phagocytes: picking the best of both worlds for tumor promotion. *Immunobiology* 211:487-501.

78. Nagaraj, S., K. Gupta, V. Pisarev, L. Kinarsky, S. Sherman, L. Kang, D. L. Herber, J. Schneck, and D. I. Gabrilovich. 2007. Altered recognition of antigen is a mechanism of CD8+ T cell tolerance in cancer. *Nat Med* 13:828-835.

79. Srivastava, M. K., P. Sinha, V. K. Clements, P. Rodriguez, and S. Ostrand-Rosenberg. 2010. Myeloid-derived suppressor cells inhibit T-cell activation by depleting cystine and cysteine. *Cancer Res* 70:68-77.

80. Hanson, E. M., V. K. Clements, P. Sinha, D. Ilkovitch, and S. Ostrand-Rosenberg. 2009. Myeloid-derived suppressor cells down-regulate L-selectin expression on CD4+ and CD8+ T cells. *J Immunol* 183:937-944.

81. Wheeler, M. C., M. Rizzi, R. Sasik, G. Almanza, G. Hardiman, and M. Zanetti. 2008. KDEL-Retained Antigen in B Lymphocytes Induces a Proinflammatory Response: A Possible Role for Endoplasmic Reticulum Stress in Adaptive T Cell Immunity. *J Immunol* 181:256-264.

82. Granados, D. P., P. L. Tanguay, M. P. Hardy, E. Caron, D. de Verteuil, S. Meloche, and C. Perreault. 2009. ER stress affects processing of MHC class I-associated peptides. *BMC Immunol* 10:10.

83. Pellicciotta, I., X. Cortez-Gonzalez, R. Sasik, Y. Reiter, G. Hardiman, P. Langlade-Demoyen, and M. Zanetti. 2008. Presentation of telomerase reverse

transcriptase, a self-tumor antigen, is down-regulated by histone deacetylase inhibition. *Cancer Res* 68:8085-8093.

84. Howarth, M., A. Williams, A. B. Tolstrup, and T. Elliott. 2004. Tapasin enhances MHC class I peptide presentation according to peptide half-life. *Proc Natl Acad Sci U S A* 101:11737-11742.

85. Mahadevan, N. R., A. Fernandez, J. Rodvold, G. Almanza, and M. Zanetti. 2010. Prostate cells undergoing ER stress in vitro and in vivo activate transcription of pro-inflammatory cytokines. *J. Inflam. Res.* 3:99-103.

86. Goodall, J. C., C. Wu, Y. Zhang, L. McNeill, L. Ellis, V. Saudek, and J. S. Gaston. 2010. Endoplasmic reticulum stress-induced transcription factor, CHOP, is crucial for dendritic cell IL-23 expression. *Proc Natl Acad Sci U S A* 107:17698-17703.

87. Chen, L., S. Jarujaron, X. Wu, L. Sun, W. Zha, G. Liang, X. Wang, E. C. Gurley, E. J. Studer, P. B. Hylemon, W. M. Pandak, Jr., L. Zhang, G. Wang, X. Li, P. Dent, and H. Zhou. 2009. HIV protease inhibitor lopinavir-induced TNF-alpha and IL-6 expression is coupled to the unfolded protein response and ERK signaling pathways in macrophages. *Biochem Pharmacol* 78:70-77.

88. Martinon, F., X. Chen, A. H. Lee, and L. H. Glimcher. 2010. TLR activation of the transcription factor XBP1 regulates innate immune responses in macrophages. *Nat Immunol* 11:411-418.

89. DeLay, M. L., M. J. Turner, E. I. Klenk, J. A. Smith, D. P. Sowders, and R. A. Colbert. 2009. HLA-B27 misfolding and the unfolded protein response augment interleukin-23 production and are associated with Th17 activation in transgenic rats. *Arthritis Rheum* 60:2633-2643.

90. Mahadevan, N. R., J. Rodvold, G. Almanza, A. Fernandez Perez, M. C. Wheeler, and M. Zanetti. 2011. ER stress activates Lipocalin 2 transcription in prostate cancer cells in an NF-kB-dependent manner. *BMC Cancer* 11:229.

91. Goetz, D. H., M. A. Holmes, N. Borregaard, M. E. Bluhm, K. N. Raymond, and R. K. Strong. 2002. The neutrophil lipocalin NGAL is a bacteriostatic agent that interferes with siderophore-mediated iron acquisition. *Mol Cell* 10:1033-1043.

92. Leng, X., T. Ding, H. Lin, Y. Wang, L. Hu, J. Hu, B. Feig, W. Zhang, L. Pusztai, W. F. Symmans, Y. Wu, and R. B. Arlinghaus. 2009. Inhibition of lipocalin 2 impairs breast tumorigenesis and metastasis. *Cancer Res* 69:8579-8584.

93. Berger, T., C. C. Cheung, A. J. Elia, and T. W. Mak. 2010. Disruption of the Lcn2 gene in mice suppresses primary mammary tumor formation but does not decrease lung metastasis. *Proc Natl Acad Sci U S A* 107:2995-3000.

94. Zhang, K., and R. J. Kaufman. 2008. From endoplasmic-reticulum stress to the inflammatory response. *Nature* 454:455-462.

95. Pikarsky, E., R. M. Porat, I. Stein, R. Abramovitch, S. Amit, S. Kasem, E. Gutkovich-Pyest, S. Urieli-Shoval, E. Galun, and Y. Ben-Neriah. 2004. NF-kappaB functions as a tumour promoter in inflammation-associated cancer. *Nature* 431:461-466.

96. Greten, F. R., L. Eckmann, T. F. Greten, J. M. Park, Z. W. Li, L. J. Egan, M. F. Kagnoff, and M. Karin. 2004. IKKbeta links inflammation and tumorigenesis in a mouse model of colitis-associated cancer. *Cell* 118:285-296.

97. Kim, S., H. Takahashi, W. W. Lin, P. Descargues, S. Grivennikov, Y. Kim, J. L. Luo, and M. Karin. 2009. Carcinoma-produced factors activate myeloid cells through TLR2 to stimulate metastasis. *Nature* 457:102-106.

98. Langowski, J. L., X. Zhang, L. Wu, J. D. Mattson, T. Chen, K. Smith, B. Basham, T. McClanahan, R. A. Kastelein, and M. Oft. 2006. IL-23 promotes tumour incidence and growth. *Nature* 442:461-465.

99. Kortylewski, M., H. Xin, M. Kujawski, H. Lee, Y. Liu, T. Harris, C. Drake, D. Pardoll, and H. Yu. 2009. Regulation of the IL-23 and IL-12 balance by Stat3 signaling in the tumor microenvironment. *Cancer Cell* 15:114-123.

100. Grivennikov, S., and M. Karin. 2008. Autocrine IL-6 signaling: a key event in tumorigenesis? *Cancer Cell* 13:7-9.

101. Thastrup, O., P. J. Cullen, B. K. Drobak, M. R. Hanley, and A. P. Dawson. 1990. Thapsigargin, a tumor promoter, discharges intracellular Ca2+ stores by specific inhibition of the endoplasmic reticulum Ca2(+)-ATPase. *Proc Natl Acad Sci U S A* 87:2466-2470.

102. Driscoll, K. E. 1994. Macrophage inflammatory proteins: biology and role in pulmonary inflammation. *Exp Lung Res* 20:473-490.

103. Kuhlicke, J., J. S. Frick, J. C. Morote-Garcia, P. Rosenberger, and H. K. Eltzschig. 2007. Hypoxia inducible factor (HIF)-1 coordinates induction of Toll-like receptors TLR2 and TLR6 during hypoxia. *PLoS ONE* 2:e1364.

104. Grivennikov, S. I., F. R. Greten, and M. Karin. 2010. Immunity, inflammation, and cancer. *Cell* 140:883-899.

105. Benson, S. A., and J. D. Ernst. 2009. TLR2-dependent inhibition of macrophage responses to IFN-gamma is mediated by distinct, gene-specific mechanisms. *PLoS One* 4:e6329.

106. Puliti, M., S. Uematsu, S. Akira, F. Bistoni, and L. Tissi. 2009. Toll-like receptor 2 deficiency is associated with enhanced severity of group B streptococcal disease. *Infect Immun* 77:1524-1531.

107. Miller, M. B., and B. L. Bassler. 2001. Quorum sensing in bacteria. *Annu Rev Microbiol* 55:165-199.

108. Qin, S., S. P. Cobbold, H. Pope, J. Elliott, D. Kioussis, J. Davies, and H. Waldmann. 1993. "Infectious" transplantation tolerance. *Science* 259:974-977.

109. Burikhanov, R., Y. Zhao, A. Goswami, S. Qiu, S. R. Schwarze, and V. M. Rangnekar. 2009. The tumor suppressor Par-4 activates an extrinsic pathway for apoptosis. *Cell* 138:377-388.

110. Gonzalez-Gronow, M., M. A. Selim, J. Papalas, and S. V. Pizzo. 2009. GRP78: a multifunctional receptor on the cell surface. *Antioxid Redox Signal* 11:2299-2306.

111. Misra, U. K., R. Deedwania, and S. V. Pizzo. 2006. Activation and cross-talk between Akt, NF-kappaB, and unfolded protein response signaling in 1-LN prostate cancer cells consequent to ligation of cell surface-associated GRP78. *J Biol Chem* 281:13694-13707.

112. Erridge, C. Endogenous ligands of TLR2 and TLR4: agonists or assistants? *J Leukoc Biol* 87:989-999.

113. Allavena, P., A. Sica, C. Garlanda, and A. Mantovani. 2008. The Yin-Yang of tumor-associated macrophages in neoplastic progression and immune surveillance. *Immunol Rev* 222:155-161.

114. Lawrence, T., and G. Natoli. 2011. Transcriptional regulation of macrophage polarization: enabling diversity with identity. *Nat Rev Immunol* 11:750-761.

115. Bronte, V., and P. Zanovello. 2005. Regulation of immune responses by L-arginine metabolism. *Nat Rev Immunol* 5:641-654.

116. Mahadevan, N. R., J. Rodvold, H. Sepulveda, S. Rossi, A. F. Drew, and M. Zanetti. 2011. Transmission of endoplasmic reticulum stress and pro-inflammation from tumor cells to myeloid cells. *Proc Natl Acad Sci U S A* 108:6561-6566.

117. Beverly, B., S. M. Kang, M. J. Lenardo, and R. H. Schwartz. 1992. Reversal of in vitro T cell clonal anergy by IL-2 stimulation. *Int Immunol* 4:661-671.

118. Filaci, G., D. Fenoglio, M. Fravega, G. Ansaldo, G. Borgonovo, P. Traverso, B. Villaggio, A. Ferrera, A. Kunkl, M. Rizzi, F. Ferrera, P. Balestra, M. Ghio, P. Contini, M. Setti, D. Olive, B. Azzarone, G. Carmignani, J. L. Ravetti, G. Torre, and F. Indiveri. 2007. CD8+ CD28- T regulatory lymphocytes inhibiting T cell proliferative and cytotoxic functions infiltrate human cancers. *J Immunol* 179:4323-4334.

119. Mahic, M., K. Henjum, S. Yaqub, B. A. Bjornbeth, K. M. Torgersen, K. Tasken, and E. M. Aandahl. 2008. Generation of highly suppressive adaptive CD8(+)CD25(+)FOXP3(+) regulatory T cells by continuous antigen stimulation. *Eur J Immunol* 38:640-646.

120. Redmond, W. L., M. J. Gough, B. Charbonneau, T. L. Ratliff, and A. D. Weinberg. 2007. Defects in the acquisition of CD8 T cell effector function after priming with tumor or soluble antigen can be overcome by the addition of an OX40 agonist. *J Immunol* 179:7244-7253.

121. Mahadevan, N. R., and M. Zanetti. 2011. Tumor stress inside out: Cell-extrinsic effects of the unfolded protein response in tumor cells modulate the immunological landscape of the tumor microenvironment. *J Immunol* 187:4403-4409.

122. Steinman, R. M., D. Hawiger, and M. C. Nussenzweig. 2003. Tolerogenic dendritic cells. *Annu Rev Immunol* 21:685-711.

123. McFarland-Mancini, M. M., H. M. Funk, A. M. Paluch, M. Zhou, P. V. Giridhar, C. A. Mercer, S. C. Kozma, and A. F. Drew. Differences in wound healing in mice with deficiency of IL-6 versus IL-6 receptor. *J Immunol* 184:7219-7228.

124. Zhang, X., R. Goncalves, and D. M. Mosser. 2008. The isolation and characterization of murine macrophages. *Curr Protoc Immunol* Chapter 14:Unit 14 11.